Structural Engineering and Mechanics, *Vol. 71, No. 5 (2019) 525-544*
DOI: https://doi.org/10.12989/sem.2019.71.5.525

Free vibration and buckling analyses of functionally graded annular thin sector plate in-plane loads using GDQM

Mehdi Mohammadimehr*[1], Hasan Afshari[1,2], M. Salemi[1], K. Torabi[1,3] and Mojtaba Mehrabi[1,3]

[1]*Department of Solid Mechanics, Faculty of Mechanical Engineering, University of Kashan, Kashan, Iran*
[2]*Department of Mechanical Engineering, Khomeinishahr Branch, Islamic Azad University, Khomeinishahr/Isfahan, Iran*
[3]*Department of Mechanics, Faculty of Engineering, University of Isfahan, Isfahan, Iran*

(Received November 21, 2018, Revised March 5, 2019, Accepted March 6, 2019)

Abstract. In the present study, buckling and free vibration analyses of annular thin sector plate made of functionally graded materials (FGMs) resting on visco-elastic Pasternak foundation, subjected to external radial, circumferential and shear in-plane loads is investigated. Material properties are assumed to vary along the thickness according to an power law with Poisson's ratio held constant. First, based on the classical plate theory (CPT), the governing equation of motion is derived using Hamilton's principle and then is solved using the generalized differential quadrature method (GDQM). Numerical results are compared to those available in the literature to validate the convergence and accuracy of the present approach. Finally, the effects of power-law exponent, ratio of radii, thickness of the plate, sector angle, and coefficients of foundation on the fundamental and higher natural frequencies of transverse vibration and critical buckling loads are considered for various boundary conditions. Also, vibration and buckling mode shapes of functionally graded (FG) sector plate have been shown in this research. One of the important obtained results from this work show that ratio of the frequency of FG annular sector plate to the corresponding values of homogeneous plate are independent from boundary conditions and frequency number.

Keywords: buckling and free vibration; annular thin sector FGM plate; visco- elastic Pasternak medium; generalized differential quadrature method

1. Introduction

Different structures such as beams, plates (Wu *et al*. (2018)), Panels (Civalek, (2008)), Carbon nanotubes (Mercan and Civalek, (2017)) and shells (Civalek, (2006)) with laminated composite (Talebitooti, (2013)) are widely used in engineering fields such as, mechanical, civil, aircrafts, automobiles, ship, petro-chemical, aeronautical, aerospace and submarine structures due to their high specific strength and low specific density (Civalek, (2013) and Baltacıoglu *et al*. (2010)). Functionally graded materials (FGMs) are inhomogeneous composite materials and their mechanical properties vary continuously in one (or more) direction(s) based on a specific function (Bourada *et al*. (2018)). The concept of functionally graded (FG) material was proposed in 1984 by the material scientists in the Sendai area of Japan (Koizumi (1997)). In the past two ten years, by using the FGM in different engineering applications, FGM structures are gaining the considerable importance and find great deal of applications in high temperature applications (Demir *et al*, (2016)). FGMs are typically made of isotropic components such as metals and ceramics. These materials used in many researches as a perfect material in micro and nano (Zemri *et al*. (2015) and Karami, (2018)) scale and came in the size-dependent (Besseghier, (2017)) and nonlocal (Bounouara *et al*. (2016), Bouafia *et al*. (2017)) analyses of different structures by Bouhadra *et al*. (2018), (2019), Hichem, (2017), Abdelaziz, (2017), Younsi, (2018), Benchohra, (2018), Yahia, (2015) and Bousahla, (2014). Also, FG materials exploit the ideal performance of their composition, e.g. heat and corrosion resistance of ceramics on one side (El-Haina, (2016)), and mechanical strength and toughness of metals on the other side of a body (Bousahla *et al.* (2016)). Many studies have been developed for static (Meski *et al*. (2019)), buckling (Akgöz and Civalek, (2011), Ghorbanpour Arani *et al*. (2011), Mohammadimehr *et al*. (2011) and Meziane, (2014)), and vibration (Mohammadimehr *et al*. (2016), (2017), Bennoun *et al*. (2016), Mohammadimehr and Shahedi (2017), Belabed *et al*. (2018) and Abualnour *et al*. (2018)), dynamic (Ghorbanpour Arani *et al*. (2011)) analyses of homogeneous or non-homogeneous plates with different shapes such as Menasria, (2017), Fourn, (2018) and Bakhadda (2018).

As a first example; static analysis of functionally graded (FG) sandwich axisymmetric annular plates is considered by Alipour (2016). He used the layer-wise and 3D elasticity theories for various elastically restrained edges under arbitrary distributed loads using a novel economical analytical solution procedure. The obtained results of his research investigated that transverse shear and normal stresses boundary conditions are exactly satisfied on the face sheets of sandwich plate and interlaminar continuity conditions of the in-plane displacement, transverse shear and normal stresses. Using differential quadrature method

*Corresponding author, Ph.D., Associate Professor
E-mail: mmohammadimehr@kashanu.ac.ir

ISSN: 1225-4568 (Print), 1598-6217 (Online)

(DQM) and Chebyshev collocation technique, Kumar and Lal (2013) predicted first three natural frequencies of free axisymmetric vibration of two directional FG annular plates resting on Winkler foundation. They investigated the effects of volume fraction index, coefficient of radial variations, exponent of the power law, foundation parameter, radius ratio and boundary condition on first three natural frequencies. Mohammadimehr and Rahmati (2013) studied the effect of small scale on electro-thermo-mechanical vibration analysis of single-walled boron nitride nanorods under electric excitation. Bhaskara and Kameswara (2014) by using classical plate theory (CPT) presented buckling analysis of elastic circular plates with elastically restrained edges and an internal elastic ring support for rotation and simply supported edges. They showed that rotational restrains effects on the buckling load is more than translational restraints of the internal elastic ring support. Based on eigenvalues and eigenfunctions problem, Yakhno and Ozdek (2014) illustrated a new analytical method for approximate computation of time-dependent Green's function for equations of the transverse vibration of a composite circular membrane with piecewise constant varying density and tension. They compared the obtained results from analytical method with experimental tests and showed that there was a good agreement with analytical and experimental outputs. Wu and Li (2017) considered three-dimensional free vibration behavior of simply supported single-layer nanoplates and graphene sheets (GSs) rested in an elastic medium using multiple time scale method based on Eringen's nonlocal elasticity theory. Their results demonstrated that natural frequencies parameters decrease when the nonlocal parameter became greater, which means the small length scales will soften the nanoplate. Powmya and Narasimhan (2015) investigated free vibration analysis of laminated, polar orthotropic, circular and annular plates based on first order shear deformation theory (FSDT) and principle collocating equations of motion at Chebyshev zeros. Their obtained results showed that transverse shear effects are more significant for polar orthotropic laminated plates than isotropic plates. Behera and Chakraverty (2015) investigated free vibration of nano beams based on Euler-Bernoulli (EBT), Timoshenko, Reddy and Levinson theories using DQM. The results of their study showed that the frequency parameter was overpredicted in EBT than other types of beam theories. Using a refined higher order exponential shear deformation theory, buckling analysis of non-axisymmetric cross-ply laminated composite plates under different boundary conditions is presented by Adim *et al*. (2016). They demonstrated that considering the refined higher order exponential shear deformation theory has strong similarity with CPT and it is simple in solving the buckling behaviors of non-axisymmetric composite plates. Thang *et al*. (2016) presented closed-form expression for nonlinear analysis of imperfect sigmoid-FGM plates with variable thickness resting on elastic medium. A new solution of free vibration response of thick-walled annular sector plates under various boundary conditions are estimated by Fadaee (2015) based on third order shear deformation theory (TSDT). Wang *et al*. (2017) investigated the micro structure dependent axisymmetric large deflection bending of pressure loaded circular FGM microplates subjected to various boundary conditions. The obtained results from their studies demonstrated that size dependent effect on the bending deflection of simply supported boundary conditions was not important against clamped boundary conditions. Dung *et al*. (2017) studied nonlinear stability of FG sandwich cylindrical shells reinforced by FGM stiffeners in thermal environment. Using finite difference discretization technique, Mehrabian and Golmakani (2015) discussed about nonlinear bending of laminated stiffened annular sector plates under mechanical loadings with various boundary conditions and orthotropic properties based on FSDT. Using finite element method (FEM) Long *et al*. (2016) developed a new eight-unknown shear deformation theory for bending and free vibration behaviors of various power-law indices FG plates. Based on the nonlocal elasticity theory, Ansari and Torabi (2016) studied vibration analysis of circular double-layered graphene sheets (DLGSs) rested in an elastic medium with Winkler spring and Pasternak shear constants in a thermal environment. Their numerical results demonstrated that the presence of elastic foundation leads to increase the fundamental frequencies of DLGSs.

Computational methods applied for vibration analysis of various structural elements can be categorized into two main groups: time-dependent methods and frequency-dependent methods (Mercan and Civalek, (2016) and Civalek, (2017)). Vibration of an annular circular plate (Xiang *et al*. (2002)) was investigated using numerical and analytical methods proposed throughout the last decades (Shirmohammadi and Bahrami, (2017)).

Recently, with increasing use of fast computers, a variety of numerical methods, i.e. FEM, the finite differences method (FDM), quadrature element method (Zhong and Yu, (2009)) and the boundary element method (BEM) are available for engineering goals. The DQM is a numerical approach for solving the differential equations which was initially introduced by Bellman *et al*. (1972). Bert and his co-workers (1972) contributed to the development of the method and used the DQM for the analysis of the structural problems. In the application of this method to the structural problems, one would meet a difficulty in implementation of the boundary conditions. Thus, this method developed and several ideas introduced to impose the boundary conditions. Also, Bert *et al*. (1966) and (1988) employed two approximate methods, which have not previously been used for structural dynamics problems. They applied these methods to the free vibration analysis of various structural components. The first method is a new version of the complementary energy method. It is shown to be considerably more accurate than the conventional Rayleigh and Rayleigh-Schmidt methods when applied to spatially one-dimensional free vibration problems: prismatic and tapered bars, prismatic beams, and axisymmetric motion of circular membranes. The second method is the DQM introduced by Bellman and his associates. Yousefitabar and Matapouri (2017) presented instability of thin annular FG CPT plates subjected to transversely distributed temperature loading. They are found that, while the temperature loading through the plate

is symmetric, first buckled configuration of a fully clamped FG plate is always asymmetric. In the other work, Mohammadimehr and Mehrabi (2017), (2018) investigated stability and free vibration analyses of double-bonded micro composite sandwich Reddy cylindrical shells conveying fluid flow based on the modified couple stress theory (MCST) and third-order shear deformation theory (TSDT) rested in an orthotropic elastic foundation under magneto-thermo-mechanical loadings using general differential quadrature method (GDQM). They concluded that the effect of static fluid flow in the both of cylindrical shells in comparison with influences of flow in the one of them was the same for the moderately thick-walled micro cylindrical shells. Satouri *et al*. (2015) studied free vibration of two dimensional (2D)-FG sectorial plate with variable thickness resting on Winkler–Pasternak elastic foundation and assumed that the plate properties vary continuously through its both circumference and thickness according to power law distribution of the volume fraction. They solved the motion equations by using the numerical DQM for various boundary conditions. Liang *et al*. (2015) showed a semi-analytical methodology for the transient response of FG annular sector plate with arbitrary circular boundary conditions. They integrated into this methodology, the state space method, DQM and the numerical inversion method of Laplace transform. They compared their results with the obtained results by FEM. It showed that the results of the present and the FEM always agree with each other excellently, regardless of which boundary condition, load and geometry are employed. Mirsalehi *et al*. (2017) illustrated the mechanical instability and free vibration of FGM micro-plate based on the modified strain gradient theory (MSGT) using the spline finite strip method. Torabi and Afshari employed differential quadrature element method (DQEM) and studied various engineering problems including vibration analysis of damaged cantilever Timoshenko beams with non-uniform cross section (Torabi *et al*, 2014a), vibration analysis of cantilever Timoshenko beams with non-uniform cross section carrying multiple concentrated elements (Torabi *et al.* (2013)), vibration analysis of rotating blades of non-uniform cross section with multiple cracks (Torabi *et al.* (2014b)) and whirling analysis of multi-span multi-stepped rotors (Afshari and Irani Rahaghi, (2018)). GDQM also can be considered as a useful tool for analyze mechanical characteristics of plates with unconventional shapes; for example Torabi and Afshari hired GDQM and investigated vibration and flutter analysis of cantilever trapezoidal plates (Torabi and Afshari, (2016) and (2017a), Afshari and Torabi, (2017), Torabi *et al*. (2017b)).

Recently, Mohammadimehr and co-workers (2016) investigated vibration and wave propagation analysis of a twisted microbeam on Pasternak foundation based on the strain gradient theory (SGT) to implement the size dependent effect. Finally, using an energy method and Hamilton's principle, they derived the governing equations of motion for the twisted micro-beam. Also, Swaminathan and Sangeetha (2017) presented a comprehensive review of developments, applications, various mathematical idealizations of materials, temperature profiles, modeling techniques and solutions methods that are adopted for the thermal analysis of FG plates.

In this article, GDQM is employed to study the free vibration and stability analysis of FG annular thin sector plate resting on visco- elastic Pasternak foundation. It is noted that in the previous papers, often analytical solutions used in order to solve the governing equations of beam, cylindrical shells and circular plates, such as alipour, (2016) and Kumar and Lal, (2013) studies. They only investigated static bending (Alipour, (2016)) and vibration analysis (Kumar and Lal, (2013)) of annular plate, While in this paper vibration and buckling analysis of a circular sector plate is performed based on a numerical method (GDQM). On the other hand, because in the most of the previous works the structures were considered resting on the elastic foundation (Ansari and Torabi, (2016) and Satouri, (2013)), in the present study, the FG thin sector annular plate assumed on viscoelastic medium to see its effects of as a completion of previous work and could be used by the other researchers. In fact, it can be said that the novelty of this research is the combining the visco-elastic thin sector annular plate with the numerical method (GDQM). The effects of the geometrical parameters of sector plate such as power-law exponent, ratio of radii, thickness of the plate and sector angle and also coefficients of foundation and in-plane loads on the fundamental and higher natural frequencies of transverse vibration and critical buckling loads are considered for various boundary conditions. Also, vibration and buckling mode shapes of functionally graded (FG) sector plate have been shown in this research.

2. Governing equation of motion

As shown in Fig. 1, a thin sector plate of inside radius b, outside radius a, thickness h and sector angle α, made of FG material is considered. The plate's material is graded through the thickness from the metal surface to the ceramic one according to a power law function as the following relations (Wang *et al*. (2017)):

$$E(z)=E_m+(E_c-E_m)\left(\frac{1}{2}+\frac{z}{h}\right)^q \quad \rho(z)=\rho_m+(\rho_c-\rho_m)\left(\frac{1}{2}+\frac{z}{h}\right)^q, \quad (1)$$

where E and ρ are modulus of elasticity and density of materials, respectively. Meanwhile, subscripts c and m are used to indicate corresponding properties in ceramic and metal, respectively. Eq. (1) can be rewritten in dimensionless form as

$$\frac{E}{E_m}=1+\left(\frac{\mu_E-1}{2^q}\right)(1+\xi)^q \quad \frac{\rho}{\rho_m}=1+\left(\frac{\mu_\rho-1}{2^q}\right)(1+\xi)^q, \quad (2)$$

in which

$$\xi=\frac{2z}{h} \quad \mu_E=\frac{E_c}{E_m} \quad \mu_\rho=\frac{\rho_c}{\rho_m}. \quad (3)$$

Let u^z, v^z and w^z be the radial, circumferential and lateral components of displacement of points at a distance z from the middle surface (z=0), respectively. Also, u, v and w be corresponding values in the midplane of the sector plate.

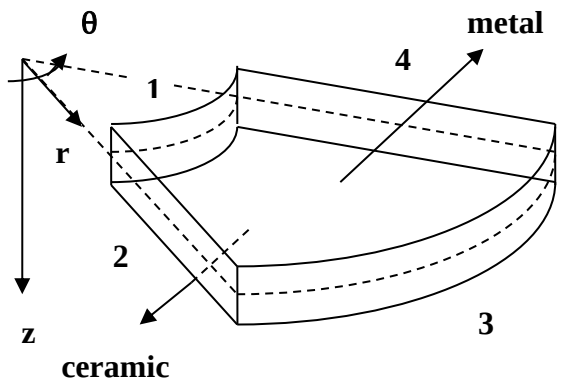

Fig. 1 A schematic of functionally graded annular sector plate

The strain-displacement relations are (Reddy, (2002))

$$\varepsilon_r=\frac{\partial u^z}{\partial r}\qquad \varepsilon_\theta=\frac{1}{r}\left(u^z+\frac{\partial v^z}{\partial\theta}\right)\qquad \varepsilon_z=\frac{\partial w^z}{\partial z}$$
$$\gamma_{r\theta}=\left(\frac{1}{r}\frac{\partial u^z}{\partial\theta}+\frac{\partial v^z}{\partial r}-\frac{v^z}{r}\right)\quad \gamma_{\theta z}=\left(\frac{\partial v^z}{\partial z}+\frac{1}{r}\frac{\partial w^z}{\partial\theta}\right)\quad \gamma_{rz}=\left(\frac{\partial u^z}{\partial z}+\frac{\partial w^z}{\partial r}\right) \tag{4}$$

where ε_r, ε_θ, ε_z, $\gamma_{r\theta}$, $\gamma_{\theta z}$ and γ_{rz} are corresponding components of strain. For thin plates ε_z, $\gamma_{\theta z}$ and γ_{rz} can be neglected. Thus, components of displacement can be written as follows:

$$u^z(r,\theta,z)=u(r,\theta)-z\frac{\partial w(r,\theta)}{\partial r}\quad v^z(r,\theta,z)=v(r,\theta)-\frac{z}{r}\frac{\partial w(r,\theta)}{\partial\theta}$$
$$w^z(r,\theta,z)=w(r,\theta) \tag{5}$$

By neglecting radial and circumferential components of displacement of the plate in midplane (Reddy 2002), displacement fields can be stated based on Kirchhoff's theory as follows:

$$u^z(r,\theta,z)=-z\frac{\partial w(r,\theta)}{\partial r}\quad v^z(r,\theta,z)=-\frac{z}{r}\frac{\partial w(r,\theta)}{\partial\theta}\quad w^z(r,\theta,z)=w(r,\theta) \tag{6}$$

Substituting Eq. (6) into the Eq. (4), following non-zero components of strain can be obtained:

$$\varepsilon_r=-z\frac{\partial^2 w}{\partial r^2}\quad \varepsilon_\theta=-\frac{z}{r}\left(\frac{\partial w}{\partial r}+\frac{1}{r}\frac{\partial^2 w}{\partial\theta^2}\right)\quad \gamma_{r\theta}=-\frac{2z}{r}\left(\frac{\partial^2 w}{\partial r\partial\theta}-\frac{1}{r}\frac{\partial w}{\partial\theta}\right) \tag{7}$$

According to the Kirchhoff's assumption, by neglecting z-component of stress in the Hook's laws, following relations can be stated

$$\sigma_r=\frac{E}{1-\upsilon^2}\left(\varepsilon_r+\upsilon\varepsilon_\theta\right)\quad \sigma_\theta=\frac{E}{1-\upsilon^2}\left(\varepsilon_\theta+\upsilon\varepsilon_r\right)\quad \sigma_{r\theta}=G\gamma_{r\theta} \tag{8}$$

In which σ_r, σ_θ and $\sigma_{r\theta}$ are radial, circumferential and in-plane components of stress, respectively. In order to derive the governing differential equations of motion, Hamilton's principle is considered as follows (Mohammadimehr *et al.* (2018))

$$\int_{t_1}^{t_2}\left(\delta U+\delta V-\delta T\right)dt=0 \tag{9}$$

where T, U, V, and δ denote the kinetic and strain energies, work done by external loads and variation operator, respectively. Also $[t_1,t_2]$ is a desired time interval.

The virtual strain energy δU is given by

$$\delta U=\iiint_{\forall}\left(\sigma_r\delta\varepsilon_r+\sigma_\theta\delta\varepsilon_\theta+\sigma_{r\theta}\delta\gamma_{r\theta}\right)d\forall \tag{10}$$

The virtual potential energy due to applied external loads δV can be stated as

$$\delta V=-\int_A F_s\delta w dA+\int_A\left[N_{rr}\frac{\partial w}{\partial r}\frac{\partial\delta w}{\partial r}+\frac{N_{\theta\theta}}{r^2}\frac{\partial w}{\partial\theta}\frac{\partial\delta w}{\partial\theta}+\frac{N_{r\theta}}{r}\left(\frac{\partial w}{\partial\theta}\frac{\partial\delta w}{\partial r}+\frac{\partial w}{\partial r}\frac{\partial\delta w}{\partial\theta}\right)\right]dA \tag{11}$$

where N_{rr}, $N_{\theta\theta}$ and $N_{r\theta}$ are external radial, circumferential and shear in-plane loads per unit length applied at the midplane of the plate, respectively and F_s is the foundation force given by Mohammadimehr *et al.* (2010) as

$$F_s=-\left(kw-G\nabla^2 w+c\frac{\partial w}{\partial t}\right) \tag{12}$$

In which k, G and c are Winkler, Pasternak and damping coefficients, respectively. The virtual kinetic energy δT is written as follows

$$\delta T=\frac{1}{2}\iiint_{\forall}\rho\delta\left[\left(\frac{\partial u^z}{\partial t}\right)^2+\left(\frac{\partial v^z}{\partial t}\right)^2+\left(\frac{\partial w^z}{\partial t}\right)^2\right]d\forall \tag{13}$$

Substituting Eqs. (10)-(13) into Eq. (9), the following relation can be derived

$$\frac{\partial^2}{\partial r^2}\left(rM_{rr}\right)-\frac{\partial M_{\theta\theta}}{\partial r}+\frac{1}{r}\frac{\partial^2 M_{\theta\theta}}{\partial\theta^2}+2\frac{\partial^2 M_{r\theta}}{\partial r\partial\theta}+\frac{2}{r}\frac{\partial M_{r\theta}}{\partial\theta}-rkw+rG\nabla^2 w-rc\frac{\partial w}{\partial t}$$
$$+\frac{\partial}{\partial r}\left(rN_{rr}\frac{\partial w}{\partial r}\right)+\frac{\partial}{\partial\theta}\left(N_{\theta\theta}\frac{1}{r}\frac{\partial w}{\partial\theta}\right)+\frac{\partial}{\partial r}\left(N_{r\theta}\frac{\partial w}{\partial\theta}\right)+\frac{\partial}{\partial\theta}\left(N_{r\theta}\frac{\partial w}{\partial r}\right) \tag{14}$$
$$-rI_0\frac{\partial^2 W}{\partial t^2}+I_2\left[\frac{\partial^3}{\partial r\partial t^2}\left(r\frac{\partial w}{\partial r}\right)+\frac{1}{r}\frac{\partial^4 w}{\partial\theta^2\partial t^2}\right]=0$$

in which I_0 and I_2 are the principal mass inertia and the rotatory inertia, respectively, defined as follows

$$\left\{I_0\quad I_2\right\}=\int_{-\frac{h}{2}}^{\frac{h}{2}}\rho(z)\left\{1\quad z^2\right\}dz=\rho_m\left\{hg_0\quad \frac{h^3 g_2}{12}\right\}, \tag{15}$$

where

$$g_0=1+\frac{\mu_\rho-1}{q+1}\quad g_2=1+\frac{3\left(\mu_\rho-1\right)\left(q^2+q+2\right)}{(q+1)(q+2)(q+3)}. \tag{16}$$

In Eq. (14), the resultant bending moments are defined as follows

$$\begin{Bmatrix}M_{rr}\\M_{\theta\theta}\\M_{r\theta}\end{Bmatrix}=\int_{-\frac{h}{2}}^{\frac{h}{2}}\begin{Bmatrix}\sigma_{rr}\\\sigma_{\theta\theta}\\\sigma_{r\theta}\end{Bmatrix}zdz=-D'\begin{Bmatrix}\frac{\partial^2 w}{\partial r^2}+\frac{\upsilon}{r}\frac{\partial w}{\partial r}+\frac{\upsilon}{r^2}\frac{\partial^2 w}{\partial\theta^2}\\ \upsilon\frac{\partial^2 w}{\partial r^2}+\frac{1}{r}\frac{\partial w}{\partial r}+\frac{1}{r^2}\frac{\partial^2 w}{\partial\theta^2}\\ (1-\upsilon)\left(\frac{1}{r}\frac{\partial^2 w}{\partial r\partial\theta}-\frac{1}{r^2}\frac{\partial w}{\partial\theta}\right)\end{Bmatrix}, \tag{17}$$

in which

$$D'=Df_2\quad D=\frac{E_m h^3}{12\left(1-\upsilon^2\right)}\quad f_2=1+\frac{3\left(\mu_E-1\right)\left(q^2+q+2\right)}{(q+1)(q+2)(q+3)} \tag{18}$$

Substituting Eq. (15) into Eq. (14), the governing differential equation can be derived as follows

$$\begin{aligned}&D'\left(\frac{\partial^4 w}{\partial r^4}+\frac{2}{r}\frac{\partial^3 w}{\partial r^3}-\frac{1}{r^2}\frac{\partial^2 w}{\partial r^2}+\frac{1}{r^3}\frac{\partial w}{\partial r}+\frac{2}{r^2}\frac{\partial^4 w}{\partial r^2\partial\theta^2}-\frac{2}{r^3}\frac{\partial^3 w}{\partial r\partial\theta^2}+\frac{4}{r^4}\frac{\partial^2 w}{\partial\theta^2}+\frac{1}{r^4}\frac{\partial^4 w}{\partial\theta^4}\right)\\&+kw-G\left(\frac{\partial^2 w}{\partial r^2}+\frac{1}{r}\frac{\partial w}{\partial r}+\frac{1}{r^2}\frac{\partial^2 w}{\partial\theta^2}\right)+c\frac{\partial w}{\partial t}-N_{rr}\left(\frac{\partial^2 w}{\partial r^2}+\frac{1}{r}\frac{\partial w}{\partial r}\right)-\frac{N_{\theta\theta}}{r^2}\frac{\partial^2 w}{\partial\theta^2}-\frac{2N_{r\theta}}{r}\frac{\partial^2 w}{\partial r\partial\theta}\\&+I_0\frac{\partial^2 W}{\partial t^2}-I_2\left(\frac{\partial^4 w}{\partial r^2\partial t^2}+\frac{1}{r}\frac{\partial^3 w}{\partial r\partial t^2}+\frac{1}{r^2}\frac{\partial^4 w}{\partial\theta^2\partial t^2}\right)=0\end{aligned} \quad (19)$$

Considering deflection of the sector plate as the product of the functions $W(\zeta,\Theta)$ which only depends on the spatial coordinates and a time dependent harmonic function as

$$w(\zeta,\Theta,t)=aW(\zeta,\Theta)e^{\omega t}, \quad (20)$$

where ω is the natural frequency; Eq. (19) can be rewritten in dimensionless form as

$$\begin{aligned}&f_2\left(\frac{\partial^4 W}{\partial\zeta^4}+2s\frac{\partial^3 W}{\partial\zeta^3}-s^2\frac{\partial^2 W}{\partial\zeta^2}+s^3\frac{\partial W}{\partial\zeta}+\frac{2s^2}{\alpha^2}\frac{\partial^4 W}{\partial\zeta^2\partial\Theta^2}-\frac{2s^3}{\alpha^2}\frac{\partial^3 W}{\partial\zeta\partial\Theta^2}+\frac{4s^4}{\alpha^2}\frac{\partial^2 W}{\partial\Theta^2}+\frac{s^4}{\alpha^4}\frac{\partial^4 W}{\partial\Theta^4}\right)\\&+k_n\beta^4 W-G_n\beta^2\left(\frac{\partial^2 W}{\partial\zeta^2}+s\frac{\partial W}{\partial\zeta}+\frac{s^2}{\alpha^2}\frac{\partial^2 W}{\partial\Theta^2}\right)+c_n\beta^4\lambda W\\&-\beta^2\left[N_{rr}^0\left(\frac{\partial^2 W}{\partial\zeta^2}+s\frac{\partial W}{\partial\zeta}\right)+N_{\theta\theta}^0\frac{s^2}{\alpha^2}\frac{\partial^2 W}{\partial\Theta^2}+2N_{r\theta}^0\frac{s}{\alpha}\frac{\partial^2 W}{\partial\zeta\partial\Theta}\right]\\&+\beta^4 g_0\lambda^2 W-\frac{\eta^2\beta^2 g_2}{12}\lambda^2\left(\frac{\partial^2 W}{\partial\zeta^2}+s\frac{\partial W}{\partial\zeta}+\frac{s^2}{\alpha^2}\frac{\partial^2 W}{\partial\Theta^2}\right)=0\end{aligned} \quad (21)$$

in which

$$\begin{aligned}&\zeta=\frac{r-b}{a-b}\quad \eta=\frac{h}{a}\quad \varphi=\frac{b}{a}\quad \beta=1-\varphi\quad \Theta=\frac{\theta}{\alpha}\quad s(\zeta)=\frac{\beta}{\beta\zeta+\phi}\quad k_n=\frac{ka^4}{D}\quad G_n=\frac{Ga^2}{D}\\&c_n=\frac{ca^2}{\sqrt{\rho_m hD}}\quad \lambda^2=\frac{\rho_m h a^4\omega^2}{D}=\frac{12(1-\upsilon^2)\rho_m a^4\omega^2}{E_m h^2}\quad N_{rr}^0=\frac{N_{rr}a^2}{D}\quad N_{\theta\theta}^0=\frac{N_{\theta\theta}a^2}{D}\quad N_{r\theta}^0=\frac{N_{r\theta}a^2}{D}\end{aligned} \quad (22)$$

3. Boundary conditions

In this article, combinations of simply supported, clamped and free edges in boundary conditions are studied. The boundary conditions (BCs) on the circular edges ($r=b,a$) can be written as

Simply supported (s): $w=0 \quad M_{rr}=0$

Clamped (c): $w=0 \quad \dfrac{\partial w}{\partial r}=0$ (1)

Free (f): $M_{rr}=0 \quad V_r=0$

And on the radial edges are:

Simply supported (s): $w=0 \quad M_{\theta\theta}=0$

Clamped (c): $w=0 \quad \dfrac{\partial w}{\partial\theta}=0$ (24)

Free (f): $M_{\theta\theta}=0 \quad V_\theta=0$

In Eqs. (23)-(24) V_r and V_θ are effective shear forces in radial and circumferential directions, respectively. Neglecting effect of the rotatory inertia on the effective shear forces, these parameters can be stated as (Reddy, (2002)):

$$\begin{aligned}V_r&=Q_r+\frac{1}{r}\frac{\partial M_{r\theta}}{\partial\theta}+N_{rr}\frac{\partial w}{\partial r}+\frac{N_{r\theta}}{r}\frac{\partial w}{\partial\theta}\\V_\theta&=Q_\theta+\frac{\partial M_{r\theta}}{\partial r}+\frac{N_{\theta\theta}}{r}\frac{\partial w}{\partial\theta}+N_{r\theta}\frac{\partial w}{\partial r}\end{aligned} \quad (24)$$

where Q_r and Q_t are shear forces in radial and circumferential directions, respectively. These terms can be defined as the following form

$$Q_r=\frac{\partial M_{rr}}{\partial r}+\frac{1}{r}\frac{\partial M_{r\theta}}{\partial\theta}+\frac{M_{rr}-M_{\theta\theta}}{r}\quad Q_\theta=\frac{\partial M_{r\theta}}{\partial r}+\frac{1}{r}\frac{\partial M_{\theta\theta}}{\partial\theta}+2\frac{M_{r\theta}}{r} \quad (25)$$

Substituting Eq. (17) and Eq. (26) into Eq. (25), the effective shear forces can be stated in terms of displacements as follows:

$$\begin{aligned}V_r&=-D'\left(\frac{\partial^3 w}{\partial r^3}+\frac{1}{r}\frac{\partial^2 w}{\partial r^2}-\frac{1}{r^2}\frac{\partial w}{\partial r}+\frac{2-\upsilon}{r^2}\frac{\partial^3 w}{\partial r\partial\theta^2}-\frac{3-\upsilon}{r^3}\frac{\partial^2 w}{\partial\theta^2}\right)+N_{rr}\frac{\partial w}{\partial r}+\frac{N_{r\theta}}{r}\frac{\partial w}{\partial\theta}\\V_\theta&=-D'\left(\frac{2-\upsilon}{r}\frac{\partial^3 w}{\partial r^2\partial\theta}-\frac{1-2\upsilon}{r^2}\frac{\partial^2 w}{\partial r\partial\theta}+\frac{2(1-\upsilon)}{r^3}\frac{\partial w}{\partial\theta}+\frac{1}{r^3}\frac{\partial^3 w}{\partial\theta^3}\right)+\frac{N_{\theta\theta}}{r}\frac{\partial w}{\partial\theta}+N_{r\theta}\frac{\partial w}{\partial r}\end{aligned} \quad (26)$$

Eqs. (17) and (27) can be rewritten in the following dimensionless forms:

$$\begin{aligned}&\frac{12(1-\upsilon^2)}{\eta E_m h^2}M_{rr}=-\frac{f_2}{\beta^2}\left(\frac{\partial^2 W}{\partial\zeta^2}+\upsilon s\frac{\partial W}{\partial\zeta}+\frac{\upsilon s^2}{\alpha^2}\frac{\partial^2 W}{\partial\Theta^2}\right)\\&\frac{12(1-\upsilon^2)}{\eta E_m h^2}M_{\theta\theta}=-\frac{f_2}{\beta^2}\left(\upsilon\frac{\partial^2 W}{\partial\zeta^2}+s\frac{\partial W}{\partial\zeta}+\frac{s^2}{\alpha^2}\frac{\partial^2 W}{\partial\Theta^2}\right)\\&\frac{12(1+\upsilon)}{\eta E_m h^2}M_{r\theta}=-\frac{f_2}{\beta^2}\left(\frac{s}{\alpha}\frac{\partial^2 W}{\partial\zeta\partial\Theta}-\frac{s^2}{\alpha}\frac{\partial W}{\partial\Theta}\right)\\&\frac{12a(1-\upsilon^2)}{\eta E_m h^2}V_r=\\&-\frac{f_2}{\beta^3}\left(\frac{\partial^3 W}{\partial\zeta^3}+s\frac{\partial^2 W}{\partial\zeta^2}-s^2\frac{\partial W}{\partial\zeta}+\frac{2-\upsilon}{\alpha^2}s^2\frac{\partial^3 W}{\partial\zeta\partial\Theta^2}-\frac{3-\upsilon}{\alpha^2}s^3\frac{\partial^2 W}{\partial\Theta^2}\right)\\&+N_{rr}^0\frac{\partial W}{\partial\zeta}+\frac{N_{r\theta}^0}{\alpha}\frac{1}{\zeta}\frac{\partial W}{\partial\Theta}\\&\frac{12a(1-\upsilon^2)}{\eta E_m h^2}V_\theta=\\&-\frac{f_2}{\beta^3}\left(\frac{2-\upsilon}{\alpha}s\frac{\partial^3 W}{\partial\zeta^2\partial\Theta}-\frac{1-2\upsilon}{\alpha}s^2\frac{\partial^2 W}{\partial\zeta\partial\Theta}+\frac{2(1-\upsilon)}{\alpha}s^3\frac{\partial W}{\partial\Theta}+\frac{s^3}{\alpha^3}\frac{\partial^3 W}{\partial\Theta^3}\right)\\&+\frac{N_{\theta\theta}^0}{\alpha}\frac{1}{\zeta}\frac{\partial W}{\partial\Theta}+N_{r\theta}^0\frac{\partial W}{\partial\zeta}\end{aligned} \quad (27)$$

4. Differential quadrature method (DQM)

According to the differential quadrature method (DQM), derivatives of a function at the point (ζ_i,Θ_i) can be expressed in terms of the value of function in throughout domain as follows:

$$\begin{cases}\left.\dfrac{d^r f}{d\zeta^r}\right|_{(\zeta,\Theta)=(\zeta_i,\Theta_j)}=\sum_{n=1}^{N}A_{in}^{(r)}f_{nj} & (i,j)=1,2,...,(N,M)\\ \left.\dfrac{d^s f}{d\Theta^s}\right|_{(\zeta,\Theta)=(\zeta_i,\Theta_j)}=\sum_{m=1}^{M}A_{jm}^{(s)}f_{im} & (r,s)=1,2,..,(N-1,M-1)\\ \left.\dfrac{\partial^{r+s} f}{\partial\zeta^r\partial\Theta^s}\right|_{(\zeta,\Theta)=(\zeta_i,\Theta_j)}=\sum_{n=1}^{N}A_{in}^{(r)}\sum_{m=1}^{M}A_{jm}^{(s)}f_{nm}\end{cases} \quad (28)$$

where $A^{(m)}$ is the weighting coefficients associated with the m^{th} order derivative and N and M are number of grid points in the ζ-direction and Θ-direction, respectively. These coefficients for the first-order derivatives are given by (Bert and Malik, (1996))

$$A_{in}^{(1)}=\begin{cases}\dfrac{\prod_{\substack{k=1\\k\neq i,n}}^{N}(\zeta_i-\zeta_k)}{\prod_{\substack{k=1\\k\neq n}}^{N}(\zeta_n-\zeta_k)}, & i,n=1,2,3,...,N;i\neq n\\ \sum_{\substack{k=1\\k\neq i}}^{N}\dfrac{1}{\zeta_i-\zeta_k}, & i=n=1,2,3,...,N\end{cases}$$

$$A_{jm}^{(1)}=\begin{cases}\dfrac{\prod_{\substack{k=1\\k\neq j,m}}^{M}(\Theta_j-\Theta_k)}{\prod_{\substack{k=1\\k\neq m}}^{M}(\Theta_m-\Theta_k)}, & j,m=1,2,3,...,M;j\neq m\\ \sum_{\substack{k=1\\k\neq j}}^{M}\dfrac{1}{\Theta_j-\Theta_k}, & j=m=1,2,3,...,M\end{cases} \tag{29}$$

and the weighting coefficients of higher-order derivatives are extracted from the following relations (Bert and Malik, (1996))

$$A_{in}^{(r)}=\begin{cases}r\left[A_{ii}^{(r-1)}A_{in}^{(1)}-\dfrac{A_{in}^{(r-1)}}{\zeta_i-\zeta_n}\right] & i,n=1,2,3,...,N;i\neq n\\ -\sum_{\substack{k=1\\k\neq i}}^{N}A_{ik}^{(r)} & i=n=1,2,3,...,N\end{cases}\quad 2\le r\le N-1$$

$$A_{jm}^{(s)}=\begin{cases}s\left[A_{jj}^{(s-1)}A_{jm}^{(1)}-\dfrac{A_{jm}^{(s-1)}}{\Theta_j-\Theta_m}\right] & j,m=1,2,3,...,M;j\neq m\\ -\sum_{\substack{k=1\\k\neq j}}^{M}A_{jk}^{(s)} & j=m=1,2,3,...,M\end{cases}\quad 2\le s\le M-1 \tag{30}$$

A convenient option for the grid points are the equally spaced points. Another choice which gives more accurate results is unequally spaced grid points (Bert and Malik, (1996)). A well-accepted set of the grid points is the Gauss–Lobatto–Chebyshev points given for interval [0,1] by

$$\zeta_i=\frac{1}{2}\left\{1-\cos\left[\frac{(i-1)\pi}{N-1}\right]\right\}\quad \Theta_j=\frac{1}{2}\left\{1-\cos\left[\frac{(j-1)\pi}{M-1}\right]\right\}. \tag{31}$$

5. Differential quadrature (DQ) analogue of governing equations

In this section, using Eq. (29), differential quadrature (DQ) forms of the governing equation and boundary conditions are obtained.

5.1 Governing Equation

Using Eq. (29) in Eq. (22) DQ form of the governing equation can be written as follows:

$$\begin{aligned}&f_2\left[\sum_{n=1}^{N}D^r{}_{in}W_{nj}+2s(\zeta_i)\sum_{n=1}^{N}C^r{}_{in}W_{nj}+s^2(\zeta_i)\left(-\sum_{n=1}^{N}B^r{}_{in}W_{nj}+\frac{2}{\alpha^2}\sum_{n=1}^{N}\sum_{m=1}^{M}B^r{}_{in}W_{nm}B^t{}_{jm}\right)\right.\\&\left.+s^3(\zeta_i)\left(\sum_{n=1}^{N}A^r{}_{in}W_{nj}-\frac{2}{\alpha^2}\sum_{n=1}^{N}\sum_{m=1}^{M}A^r{}_{in}W_{nm}B^t{}_{jm}\right)+\frac{s^4(\zeta_i)}{\alpha^2}\left(4\sum_{m=1}^{M}B^t{}_{jm}W_{im}+\frac{1}{\alpha^2}\sum_{m=1}^{M}D^t{}_{jm}W_{im}\right)\right]\\&+k_n\beta^4W_{ij}-G_n\beta^2\left[\sum_{n=1}^{N}B^r{}_{in}W_{nj}+s(\zeta_i)\sum_{n=1}^{N}A^r{}_{in}W_{nj}+\frac{s^2(\zeta_i)}{\alpha^2}\sum_{m=1}^{M}B^t{}_{jm}W_{im}\right]+c_n\beta^4\lambda W_{ij}\\&+\beta^2\left\{N_{rr}^0\left[\sum_{n=1}^{N}B^r{}_{in}W_{nj}+s(\zeta_i)\sum_{n=1}^{N}A^r{}_{in}W_{nj}\right]+\frac{N_{\theta\theta}^0s^2(\zeta_i)}{\alpha^2}\sum_{m=1}^{M}B^t{}_{jm}W_{im}+2\frac{N_{r\theta}^0s(\zeta_i)}{\alpha}\sum_{n=1}^{N}\sum_{m=1}^{M}A^r{}_{in}W_{nm}A^t{}_{jm}\right\}\\&+\lambda^2\left\{\beta^4g_0W_{ij}-\frac{\eta^2\beta^2g_2}{12}\left[\sum_{n=1}^{N}B^r{}_{in}W_{nj}+s(\zeta_i)\sum_{n=1}^{N}A^r{}_{in}W_{nj}+\frac{s^2(\zeta_i)}{\alpha^2}\sum_{m=1}^{M}B^t{}_{jm}W_{im}\right]\right\}=0,\end{aligned} \tag{32}$$

where

$$W_{ij}=W(\zeta_i,\Theta_j) \tag{33}$$

5.1.1 Vibration analysis

For vibration analysis, Eq. (33) can be written using Kronecker product as follows

$$[Q_v]\{\hat{W}\}+c_n\beta^4\lambda\{\hat{W}\}+\lambda^2[P]\{\hat{W}\}=0, \tag{34}$$

in which following column vector is defined

$$\hat{W}_k=W_{ij}\quad k=(j-1)N+i, \tag{35}$$

and

$$\begin{aligned}Q_v=&f_2\left(I_M\otimes\left\{[D^r]+2[s][C^r]-[s]^2[B^r]+[s]^3[A^r]\right\}\right.\\&\left.+\frac{1}{\alpha^2}[B^t]\otimes\left\{2[s]^2[B^r]-2[s]^3[A^r]+4[s]^4\right\}+\frac{1}{\alpha^4}[D^t]\otimes[s]^4\right)\\&+k_n\beta^4I_M\otimes I_N-G_n\beta^2\left[I_M\otimes\left([B^r]+[s][A^r]\right)+\frac{1}{\alpha^2}[B^t]\otimes[s]^2\right]\\&-\beta^2\left\{N_{rr}^0\left[I_M\otimes\left([B^r]+[s][A^r]\right)\right]+\frac{N_{\theta\theta}^0}{\alpha^2}[B^t]\otimes[s]^2+2\frac{N_{r\theta}^0}{\alpha}[A^t]\otimes[s][A^r]\right\}\\P=&\beta^4g_0I_M\otimes I_N-\frac{\eta^2\beta^2g_2}{12}\left\{I_M\otimes\left([B^r]+[s][A^r]\right)+\frac{1}{\alpha^2}[B^t]\otimes[s]^2\right\}\end{aligned} \tag{36}$$

where I_N and I_M are identity matrix of size N and M, respectively. In order to eliminating the redundant equations, motion equations should be represented only for domain points (Bert *et al*. 1988). Thus:

$$[\bar{Q}_v]\{\hat{W}\}+c_n\beta^4\lambda\{\hat{W}\}_d+\lambda^2[\bar{P}]\{\hat{W}\}=0, \tag{37}$$

thickness in which bar sign shows the corresponding truncated non-square matrices. Eq. (38) may be rearranged and partitioned in order to separate the boundary and domain components as:

$$\begin{aligned}&[\bar{Q}_v]_b\{\hat{W}\}_b+[\bar{Q}_v]_d\{\hat{W}\}_d+c_n\beta^4\lambda\{\hat{W}\}_d\\&+\lambda^2\left([\bar{P}]_b\{\hat{W}\}_b+[\bar{P}]_d\{\hat{W}\}_d\right)=0,\end{aligned} \tag{38}$$

where

$$\{\hat{W}\}_b=\left\{\begin{bmatrix}W_{11}\\W_{21}\\\cdot\\\cdot\\\cdot\\W_{(N-1)1}\\W_{N1}\end{bmatrix}^T\begin{bmatrix}W_{12}\\W_{22}\\\cdot\\\cdot\\\cdot\\W_{(N-1)2}\\W_{N2}\end{bmatrix}^T\begin{bmatrix}W_{13}\\W_{23}\\W_{(N-1)3}\\W_{N3}\end{bmatrix}^T\begin{bmatrix}W_{14}\\W_{24}\\W_{(N-1)4}\\W_{N4}\end{bmatrix}^T\ \cdots\ \begin{bmatrix}W_{1(M-3)}\\W_{2(M-3)}\\W_{(N-1)(M-3)}\\W_{N(M-3)}\end{bmatrix}^T\begin{bmatrix}W_{1(M-2)}\\W_{2(M-2)}\\W_{(N-1)(M-2)}\\W_{N(M-2)}\end{bmatrix}^T\begin{bmatrix}W_{1(M-1)}\\W_{2(M-1)}\\\cdot\\\cdot\\\cdot\\W_{(N-1)(M-1)}\\W_{N(M-1)}\end{bmatrix}^T\begin{bmatrix}W_{1M}\\W_{2M}\\\cdot\\\cdot\\\cdot\\W_{(N-1)M}\\W_{NM}\end{bmatrix}^T\right\}^T. \tag{39}$$

$$\left\{\hat{W}\right\}_d = \left\{ \begin{bmatrix} W_{33} \\ W_{43} \\ . \\ . \\ . \\ W_{(N-3)3} \\ W_{(N-2)3} \end{bmatrix}^T \begin{bmatrix} W_{34} \\ W_{44} \\ . \\ . \\ . \\ W_{(N-3)4} \\ W_{(N-2)4} \end{bmatrix}^T \ ... \ \begin{bmatrix} W_{3(M-3)} \\ W_{4(M-3)} \\ . \\ . \\ . \\ W_{(N-3)(M-3)} \\ W_{(N-2)(M-3)} \end{bmatrix}^T \begin{bmatrix} W_{3(M-2)} \\ W_{4(M-2)} \\ . \\ . \\ . \\ W_{(N-3)(M-2)} \\ W_{(N-2)(M-2)} \end{bmatrix}^T \right\}^T \quad (40)$$

5.1.2 Stability analysis

In order to stability analysis, in Eq. (33) value of the frequency should be considered as zero; By definition critical loads as:

$$N_{rr}^{cr} = -N_{rr}^0 \quad N_{\theta\theta}^{cr} = -N_{\theta\theta}^0 \quad N_{r\theta}^{cr} = N_{r\theta}^0 \quad (41)$$

Eq. (33) can be written for buckling of the plate under radial, circumferential or shear loads as:

$$\left[Q_s\right]\left\{\hat{W}\right\} = -\beta^2 N_{kl}^{cr}\left[P_{kl}\right]\left\{\hat{W}\right\} \quad k = r,\theta \quad l = r,\theta, \quad (42)$$

where

$$\begin{aligned} Q_s &= f_2\left(I_M \otimes \left\{\left[D^r\right] + 2[s]\left[C^r\right] - [s]^2\left[B^r\right] + [s]^3\left[A^r\right]\right\}\right. \\ &+ \frac{1}{\alpha^2}\left[B^t\right] \otimes \left\{2[s]^2\left[B^r\right] - 2[s]^3\left[A^r\right] + 4[s]^4\right\} + \frac{1}{\alpha^4}\left[D^r\right] \otimes [s]^4\Big) \\ &+ k_n\beta^4 I_M \otimes I_N - G_n\beta^2\left[I_M \otimes \left(\left[B^r\right] + [s]\left[A^r\right]\right) + \frac{1}{\alpha^2}\left[B^t\right] \otimes [s]^2\right] \\ \left[P_{rr}\right] &= I_M \otimes \left(\left[B^r\right] + [s]\left[A^r\right]\right) \quad \left[P_{\theta\theta}\right] = \frac{1}{\alpha^2}\left[B^t\right] \otimes [s]^2 \quad \left[P_{r\theta}\right] = \frac{-2}{\alpha}\left[A^t\right] \otimes [s]\left[A^r\right] \end{aligned} \quad (43)$$

In a similar manner with vibration analysis, Eq. (38) may be rearranged and partitioned in order to separate the boundary and domain components as

$$\begin{aligned} &\left[\bar{Q}_s\right]_b \left\{\hat{W}\right\}_b + \left[\bar{Q}_s\right]_d \left\{\hat{W}\right\}_d \\ &= -\beta^2 N_{kl}^{cr}\left(\left[\bar{P}_{kl}\right]_b \left\{\hat{W}\right\}_b + \left[\bar{P}_{kl}\right]_d \left\{\hat{W}\right\}_d\right). \end{aligned} \quad (44)$$

5.2 Boundary conditions

Before implying boundary conditions, DQ form of Eq. (28) should be written as follows

$$\begin{aligned} \frac{12(1-\upsilon^2)}{\eta E_m h^2}\{M_{rr}\}_{ij} &= -\frac{f_2}{\beta^2}\left[\sum_{n=1}^{N} B^r{}_{in} W_{nj} + \upsilon s(\zeta_i)\left(\sum_{n=1}^{N} A^r{}_{in} W_{nj} + \frac{s(\zeta_i)}{\alpha^2}\sum_{m=1}^{M} B^t{}_{jm} W_{im}\right)\right] \\ \frac{12(1-\upsilon^2)}{\eta E_m h^2}\{M_{\theta\theta}\}_{ij} &= -\frac{f_2}{\beta^2}\left[\upsilon\sum_{n=1}^{N} B^r{}_{in} W_{nj} + s(\zeta_i)\left(\sum_{n=1}^{N} A^r{}_{in} W_{nj} + \frac{s(\zeta_i)}{\alpha^2}\sum_{m=1}^{M} B^t{}_{jm} W_{im}\right)\right] \\ \frac{12(1+\upsilon)}{\eta E_m h^2}\{M_{r\theta}\}_{ij} &= -\frac{f_2}{\beta^2}\frac{s(\zeta_i)}{\alpha}\left(\sum_{n=1}^{N}\sum_{m=1}^{M} A^r{}_{in} W_{nm} A^t{}_{jm} - s(\zeta_i)\sum_{m=1}^{M} A^t{}_{jm} W_{im}\right) \\ \frac{12a(1-\upsilon^2)}{\eta E_m h^2}\{V_r\}_{ij} &= -\frac{f_2}{\beta^3}\left[\sum_{n=1}^{N} C^r{}_{in} W_{nj} + s(\zeta_i)\sum_{n=1}^{N} B^r{}_{in} W_{nj}\right. \\ &+ s^2(\zeta_i)\left(\frac{2-\upsilon}{\alpha^2}\sum_{n=1}^{N}\sum_{m=1}^{M} A^r{}_{in} W_{nm} B^t{}_{jm} - \sum_{n=1}^{N} A^r{}_{in} W_{nj}\right) - \frac{3-\upsilon}{\alpha^2} s^3(\zeta_i)\sum_{m=1}^{M} B^t{}_{jm} W_{im}\Big] \\ &+ N_{rr}^0\sum_{n=1}^{N} A^r{}_{in} W_{nj} + \frac{N_{r\theta}^0}{\alpha} s(\zeta_i)\sum_{m=1}^{M} A^t{}_{jm} W_{im} \\ \frac{12a(1-\upsilon^2)}{\eta E_m h^2}\{V_\theta\}_{ij} &= -\frac{f_2}{\beta^3}\left\{\frac{2-\upsilon}{\alpha} s\sum_{n=1}^{N}\sum_{m=1}^{M} B^r{}_{in} W_{nm} A^t{}_{jm} - \frac{1-2\upsilon}{\alpha} s^2\sum_{n=1}^{N}\sum_{m=1}^{M} A^r{}_{in} W_{nm} A^t{}_{jm}\right. \\ &+ \frac{s^3}{\alpha}\left[2(1-\upsilon)\sum_{m=1}^{M} A^t{}_{jm} W_{im} + \frac{1}{\alpha^2}\sum_{m=1}^{M} C^t{}_{jm} W_{im}\right]\Big\} + \frac{N_{\theta\theta}^0}{\alpha} s(\zeta_i)\sum_{m=1}^{M} A^t{}_{jm} W_{im} + N_{r\theta}^0\sum_{n=1}^{N} A^r{}_{in} W_{nj} \end{aligned} \quad (45)$$

where

$$\begin{gathered} \{M_{rr}\}_{ij} = M_{rr}(\zeta_i,\Theta_j) \quad \{M_{\theta\theta}\}_{ij} = M_{\theta\theta}(\zeta_i,\Theta_j) \quad \{M_{r\theta}\}_{ij} = M_{r\theta}(\zeta_i,\Theta_j) \\ \{V_r\}_{ij} = V_r(\zeta_i,\Theta_j) \quad \{V_\theta\}_{ij} = V_\theta(\zeta_i,\Theta_j) \end{gathered} \quad (46)$$

Eq. (44) can be rewritten using Kronecker product as

$$\begin{aligned} \frac{12(1-\upsilon^2)}{\eta E_m h^2}\{\hat{M}_{rr}^3\} &= -\frac{f_2}{\beta^2}\left[I_M \otimes \left\{\left[B^r\right] + \upsilon[s]\left[A^r\right]\right\} + \frac{\upsilon}{\alpha^2}\left\{\left[B^t\right] \otimes [s]^2\right\}\right]\{W\} \\ \frac{12(1-\upsilon^2)}{\eta E_m h^2}\{\hat{M}_{\theta\theta}^3\} &= -\frac{f_2}{\beta^2}\left[I_M \otimes \left\{\upsilon\left[B^r\right] + [s]\left[A^r\right]\right\} + \frac{1}{\alpha^2}\left\{\left[B^t\right] \otimes [s]^2\right\}\right]\{W\} \\ \frac{12(1+\upsilon)}{\eta E_m h^2}\{\hat{M}_{r\theta}^3\} &= -\frac{f_2}{\beta^2\alpha}\left\{\left[A^t\right] \otimes [s]\left\{\left[A^r\right] - [s]\right\}\right\}\{W\} \\ \frac{12a(1-\upsilon^2)}{\eta E_m h^2}\{\hat{V}_r\} &= -\frac{f_2}{\beta^3}\left(I_M \otimes \left\{\left[C^r\right] + [s]\left[B^r\right] - [s]^2\left[A^r\right]\right\}\right. \\ &+ \frac{2-\upsilon}{\alpha^2}\left\{\left[B^t\right] \otimes [s]^2\left[A^r\right]\right\} - \frac{3-\upsilon}{\alpha^2}\left\{\left[B^t\right] \otimes [s]^3\right\}\Big)\{\hat{W}^3\} + \left\{N_{rr}^0 I_M \otimes \left[A^r\right] + \frac{N_{r\theta}^0}{\alpha}\left[A^t\right] \otimes [s]\right\}\{W\} \\ \frac{12a(1-\upsilon^2)}{\eta E_m h^2}\{\hat{V}_\theta^3\} &= -\frac{f_2}{\beta^3}\left(\frac{\left[A^t\right]}{\alpha} \otimes \left\{(2-\upsilon)[s]\left[B^r\right] - (1-2\upsilon)[s]^2\left[A^r\right] + 2(1-\upsilon)[s]^3\right\} + \frac{1}{\alpha^3}\left[C^t\right] \otimes [s]^3\right)\{W\} \\ &+ \left\{N_{r\theta}^0 I_M \otimes \left[A^r\right] + \frac{N_{\theta\theta}^0}{\alpha}\left[A^t\right] \otimes [s]\right\}\{\hat{W}\} \end{aligned} \quad (47)$$

in which following column vectors are defined

$$\begin{gathered} \left\{\hat{M}_{rr}\right\}_k = \{M_{rr}\}_{ij} \quad \left\{\hat{M}_{\theta\theta}\right\}_k = \{M_{\theta\theta}\}_{ij} \quad \left\{\hat{M}_{r\theta}\right\}_k = \{M_{r\theta}\}_{ij} \quad \left\{\hat{V}_r\right\}_k = \{V_r\}_{ij} \quad \left\{\hat{V}_\theta\right\}_k = \{V_\theta\}_{ij} \\ k = (j-1)N + i \end{gathered} \quad (48)$$

Each boundary condition contains constrains on the transverse deflection, slope, bending moment or effective shear force written as

$$\left[T\right]\left\{\hat{W}\right\} = 0 \quad (49)$$

Eq. (50) may be rearranged and partitioned in order to separate the boundary and domain components as

$$\left[T\right]_b \left\{\hat{W}\right\}_b + \left[T\right]_d \left\{\hat{W}\right\}_d = 0 \quad (50)$$

Substituting Eq. (51) into Eq. (43), following eigenvalue equation can be obtained for stability analysis

$$\left[X_s\right]\left\{\hat{W}\right\}_d = -\beta^2 N_{kl}^{cr}\left[Y_s\right]\left\{\hat{W}\right\}_d \quad (51)$$

where

$$\begin{aligned} \left[X_s\right] &= \left[\bar{Q}_s\right]_d - \left[\bar{Q}_s\right]_b \left[T\right]_b^{-1}\left[T\right]_d \\ \left[Y_s\right] &= \left[\bar{P}_{kl}\right]_d - \left[\bar{P}_{kl}\right]_b \left[T\right]_b^{-1}\left[T\right]_d \end{aligned} \quad (52)$$

According to Eq. (25), this procedure cannot be followed for cases whose boundary conditions contains free edge(s).

Using Eq. (51) in Eq. (39), following eigenvalue equation can be obtained for vibration analysis

$$\left[X_v\right]\left\{\hat{W}\right\}_d + c_n\beta^4\lambda\left\{\hat{W}\right\}_d + \lambda^2\left[Z_v\right]\left\{\hat{W}\right\}_d = 0 \quad (53)$$

where

$$\begin{aligned} \left[X_v\right] &= \left[\bar{Q}_v\right]_d - \left[\bar{Q}_v\right]_b \left[T\right]_b^{-1}\left[T\right]_d \\ \left[Z_v\right] &= \left[\bar{P}\right]_d - \left[\bar{P}\right]_b \left[T\right]_b^{-1}\left[T\right]_d \end{aligned} \quad (54)$$

By introducing following vector

$$\{\Psi\} = \begin{Bmatrix} \left\{\hat{W}\right\}_d \\ \lambda\left\{\hat{W}\right\}_d \end{Bmatrix} \quad (55)$$

Eq. (54) can be replaced by a standard eigenvalue problem as

$$\left[K_f\right]\{\Psi\} = \lambda\left[M_f\right]\{\Psi\}, \quad (56)$$

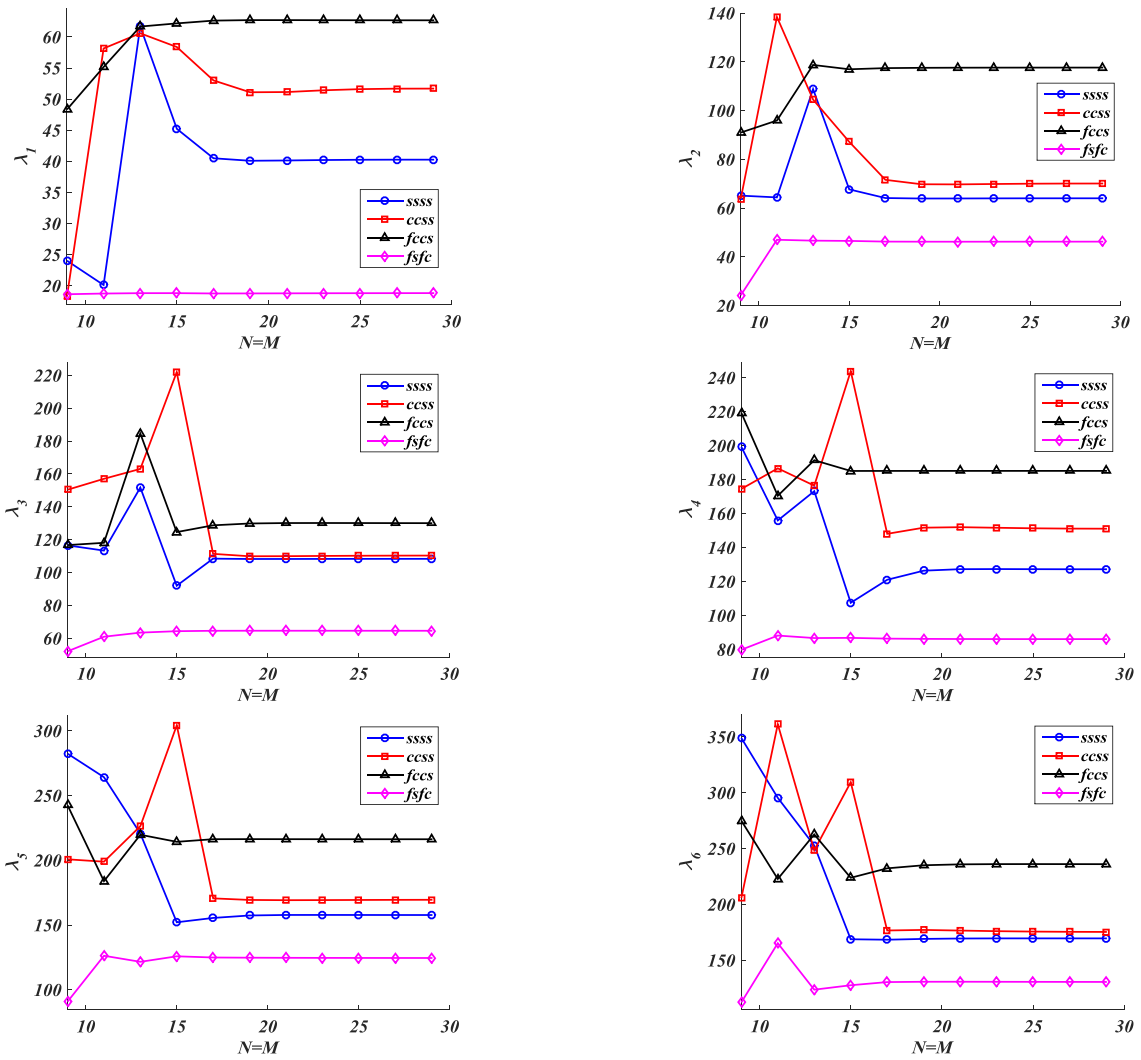

Fig. 2. Convergence of the presented solution in first six modes (q=1, φ=0.3, α=π/2, η=0.05, k_n=G_n=10, c_n=0, N_{rr}=N_{tt}=N_{rt}=10)

where

$$\left[K_f\right]=\begin{bmatrix}-\left[X_v\right] & -c_n\beta^4 I_p\\ \{0\}_p & I_p\end{bmatrix}\quad \left[M_f\right]=\begin{bmatrix}\{0\}_p & [Z_v]\\ I_p & \{0\}_p\end{bmatrix} \tag{57}$$

$$p=MN-4(M+N)+16$$

6. Numerical results

In this section numerical results are presented for various cases. Results are presented for FG plates made of *Ni* (as metal) and Al_2O_3 (as ceramic) with the properties presented in Table 1. Also, Posisson's ratio is considered as υ=0.3. It is worth mentioning that boundary conditions are numbered according to numbers assigned to each edge in Fig. 1.

For FG plates with different boundary conditions, the effect of the number of grid points (N=M) on the dimensionless values of the natural frequency of first four modes are depicted in Fig. 2. As shown in this figure presented solution is convergent in all combination of boundary conditions. In what follows, results are reported for N=M=19.

Table 1 Material properties of metal and ceramic (Cho and Oden, 2000)

Properties	Metal (Ni)	ceramic (Al_2O_3)
Modulus of elasticity (GPa)	199.5	393
Density (kg/m^3)	8900	3970

In order to confirm accuracy of the proposed solution a homogenous annular sector plate with simply supported radial edges (Kim and Dickinson, (1989)) is considered. Table 2 shows the lowest four dimensionless frequencies (λ) for various cases in boundary conditions of circular edges. According to this table, the presented results are in excellent agreement with those reported by Kim and Dickinson (1989) based on the Rayleigh-Ritz method. It should be noted that Kim and Dickinson (1989) neglected rotary inertia, so in this table results are presented for a small value of η.

It is worth mentioning that many numerical approaches like finite element method (FEM), Rayleigh-Ritz method, Galerkin method and differential transform method (DTM) need to integral operation and it makes them too time-consuming (Afshari and Irani Rahaghi, (2018)). Also, some

Table 2 First four dimensionless natural frequencies of homogeneous annular sector plates (φ=0.2, α=π/3, ν=0.3, η=0.0001, k_n=0, G_n=0, c_n=0, N_{rr}= $N_{\theta\theta}$= $N_{r\theta}$=0)

		Mode 1	Mode 2	Mode 3	Mode 4
FSFS	Present	12.4229	47.3836	52.4489	102.1073
	Kim and Dickinson, (1989)	12.40	47.38	52.47	102.1
FSSS	Present	39.6545	92.6784	97.9922	162.9927
	Kim and Dickinson, (1989)	39.66	92.68	97.99	163
FSCS	Present	50.449	108.6301	114.1272	184.1136
	Kim and Dickinson, (1989)	50.51	108.4	114.2	183.3
SSFS	Present	12.5022	47.3828	53.6651	102.1089
	Kim and Dickinson, (1989)	12.47	47.38	53.7	102.1
SSSS	Present	40.2712	97.4852	97.9804	177.1823
	Kim and Dickinson, (1989)	40.31	97.52	98	177.6
SSCS	Present	51.6672	114.2143	115.3345	198.3216
	Kim and Dickinson, (1989)	51.7	114.2	115.4	198.8
CSFS	Present	12.5756	47.3655	55.4678	102.1072
	Kim and Dickinson, (1989)	12.61	47.38	55.41	102.1
CSSS	Present	41.4165	98.0153	102.2578	177.1837
	Kim and Dickinson, (1989)	41.33	98	102.4	177.6
CSCS	Present	53.4162	144.2379	121.7530	198.3220
	Kim and Dickinson, (1989)	53.39	144.2	121.7	198.8

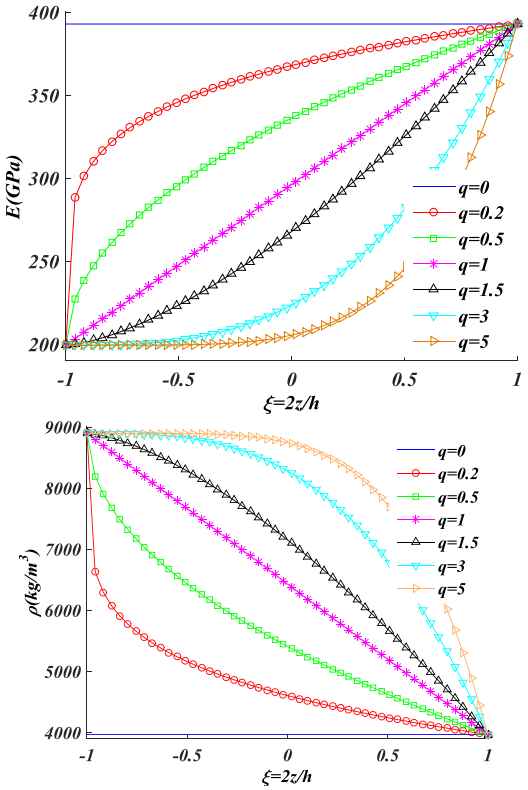

Fig. 3 Distribution of elasticity modulus and mass density through the thickness for various values of q

Table 3 First three dimensionless natural frequencies of FG sector plate for some boundary conditions and various values of q (φ=0.3, α=π/3, η=0.05, k_n=0, G_n=0, c_n=0, N_{rr}=$N_{\theta\theta}$=$N_{r\theta}$=0)

SSSS						
q	λ_1	λ_2	λ_3	λ_4	λ_5	λ_6
0	87.68716	203.9808	224.8771	366.5062	382.1282	433.7152
0.2	75.67697	176.0031	194.0266	316.1404	329.6062	374.0695
0.5	66.65008	155.0140	170.8890	278.4513	290.3130	329.4799
1	59.79844	139.1051	153.3554	249.9397	260.5931	295.773
1.5	56.46105	131.3620	144.8225	236.0772	246.1446	279.3912
3	52.04373	121.1105	133.5249	217.7172	227.0078	257.6916
5	49.51072	115.2214	127.0332	207.1443	215.9850	245.1836
CSCS						
q	λ_1	λ_2	λ_3	λ_4	λ_5	λ_6
0	125.5506	238.7432	300.6602	409.8043	437.455	550.2541
0.2	108.3525	205.9924	259.4018	353.4766	377.3158	474.5482
0.5	95.42822	181.4276	228.4696	311.3379	332.3366	417.9855
1	85.61948	162.8114	205.0358	279.4669	298.3234	375.2469
1.5	80.84199	153.7513	193.6332	263.9728	281.7895	354.4808
3	74.51843	141.7559	178.5353	243.4511	259.8899	326.9713
5	70.89183	134.8637	169.8569	231.6301	247.2722	311.1053
CFSC						
q	λ_1	λ_2	λ_3	λ_4	λ_5	λ_6
0	71.24048	146.0303	218.0415	281.5541	318.2204	443.948
0.2	61.48788	126.0251	188.1479	242.9253	274.5468	382.9375
0.5	54.15287	110.9931	165.7089	213.9568	241.8093	337.2855
1	48.58259	99.58566	148.6939	192.0064	217.0111	302.7513
1.5	45.86860	94.02978	140.4103	181.3243	204.9454	285.9609
3	42.27674	86.67581	129.4443	167.1811	188.9692	263.723
5	40.21841	82.45779	123.1483	159.0535	179.7843	250.9162
SFFC						
q	λ_1	λ_2	λ_3	λ_4	λ_5	λ_6
0	13.09325	53.62929	76.76795	179.9553	222.5286	343.9605
0.2	11.30188	46.29101	66.25924	155.3041	192.0303	296.7626
0.5	9.953528	40.76845	58.35498	136.7795	169.127	261.3751
1	8.928970	36.57261	52.35207	122.7209	151.7538	234.5646
1.5	8.429617	34.52777	49.4272	115.8735	143.2945	221.5185
3	7.768817	31.82175	45.55629	106.8102	132.0964	204.2447
5	7.390425	30.27196	43.33820	101.6121	125.6699	194.3162

of them need to admissible functions which are not available for some combination of boundary conditions. GDQM converts differential equation to an equivalent algebraic system of equations which is less time-consuming in comparison with above mentioned numerical methods and it is the main reason for authors to choose this numerical method

Table 3 presents the value of the first three natural frequencies for various values of power-law exponent (*q*). As shown in this table, the values of the all frequencies

Table 4 First six natural frequencies of FG sector plate for some boundary conditions and various values of the ratio of inner radius to outer radius (q=1, α=π/3, η=0.05, k_n=0, G_n=0, c_n=0, $N_{rr}=N_{\theta\theta}=N_{r\theta}$=0)

	φ					φ				
	0.2	0.35	0.5	0.65	0.8	0.2	0.35	0.5	0.65	0.8
			λ_1					λ_2		
CCCC	107.9169	114.1746	151.0405	273.6194	786.1806	207.3602	211.1418	225.6242	322.2992	815.4148
SFSF	22.71056	33.60341	56.15057	113.8614	343.5715	43.19545	52.70108	73.3892	128.9942	356.0820
FCFS	28.18914	28.07643	27.23989	25.14786	22.07486	87.22974	83.93159	80.15924	80.12216	74.34077
SCCS	89.59816	93.40354	117.4830	200.8038	555.1901	180.6605	185.6399	194.2937	257.2116	593.9137
SSFS	17.87429	18.29358	20.10083	25.63656	43.30435	67.67842	67.6895	68.11921	72.28581	96.83541
FCSC	86.11596	86.75239	81.43751	72.84799	78.38543	125.0839	170.3379	161.1926	167.8737	168.8615
			λ_3					λ_4		
CCCC	210.748	244.9321	345.2892	410.3125	867.4346	338.3199	341.8672	370.3755	537.2904	945.4887
SFSF	87.90647	110.0525	125.3257	176.4963	398.5875	106.9391	132.2547	211.7457	253.8962	467.7817
FCFS	92.42914	89.37469	85.24898	83.85605	111.4689	171.8520	197.7925	168.3138	166.7883	155.9104
SCCS	187.1361	211.0542	309.9721	352.5015	660.2399	304.1410	309.2529	312.3023	483.5947	755.3218
SSFS	76.59384	85.27862	114.4634	147.4523	172.1221	145.2119	145.2121	145.2778	200.1428	271.6170
FCSC	182.0540	183.4890	181.2291	226.0094	282.5007	183.5397	270.8641	297.7219	294.8528	422.5825
			λ_5					λ_6		
CCCC	341.9944	358.7864	443.2165	698.6306	1051.804	351.7568	436.3425	499.2020	710.3138	1186.864
SFSF	120.9903	157.3217	221.7576	362.0457	562.9763	195.3347	205.4961	241.8891	445.9221	683.4520
FCFS	182.0962	280.3728	183.7474	180.1072	225.5711	202.5584	285.4316	191.2264	278.3223	265.8007
SCCS	309.4246	325.2642	388.4482	585.8907	879.1489	322.0097	387.5521	460.2212	639.8285	1030.310
SSFS	164.9899	174.8430	190.5357	249.8975	395.6439	173.7467	203.7651	248.9443	265.7500	543.4669
FCSC	293.2176	308.0842	307.5305	327.5277	570.998	308.1393	316.056	335.8858	449.9125	589.2373

Table 5 First six natural frequencies of FG sector plate for some boundary conditions and various values of sector angle (q=1, φ=0.3, η=0.05, k_n=0, G_n=0, c_n=0, $N_{rr}=N_{\theta\theta}=N_{r\theta}$=0)

	α					α				
	π/6	π/3	π/2	2π/3	π	π/6	π/3	π/2	2π/3	π
			λ_1					λ_2		
SSSS	139.1051	59.79844	43.24999	37.43206	33.33858	260.5931	139.1051	81.9745	59.79844	43.24999
CSCS	162.8114	85.61948	73.02566	69.16845	66.65796	298.3234	162.8114	105.2831	85.61948	73.02566
CCFC	145.9804	40.24125	19.96302	13.5196	10.2112	278.0886	103.0003	48.28978	28.61967	14.93389
FSSS	138.9076	55.33666	34.47104	25.90009	18.34432	256.9438	126.3340	80.13399	55.33666	34.47104
			λ_3					λ_4		
SSSS	387.4693	153.3554	132.6089	94.80982	59.79844	413.4524	249.9397	139.1051	125.3873	81.97459
CSCS	423.1554	205.0358	162.8114	117.6207	85.61948	472.9878	279.4669	189.5151	162.8116	105.2832
CCFC	384.7309	112.1142	79.87236	52.95229	25.17241	429.1788	194.4231	90.83694	70.52016	39.67382
FSSS	387.4692	138.9076	92.65823	78.08015	55.33666	391.876	226.6484	138.9076	93.70433	65.44466
			λ_5					λ_6		
SSSS	592.3029	260.5931	182.2421	139.1053	108.6608	606.2487	295.7730	209.9052	153.3554	120.2571
CSCS	636.2839	298.3234	228.1704	184.3451	131.4317	692.1029	375.2469	237.3374	205.0358	162.7490
CCFC	603.3879	222.6986	131.7742	84.73651	57.68649	620.2252	226.3481	145.7410	98.77285	64.64246
FSSS	545.1456	249.936	166.0006	126.3340	80.13408	592.2986	256.9438	188.4585	138.9078	92.65823

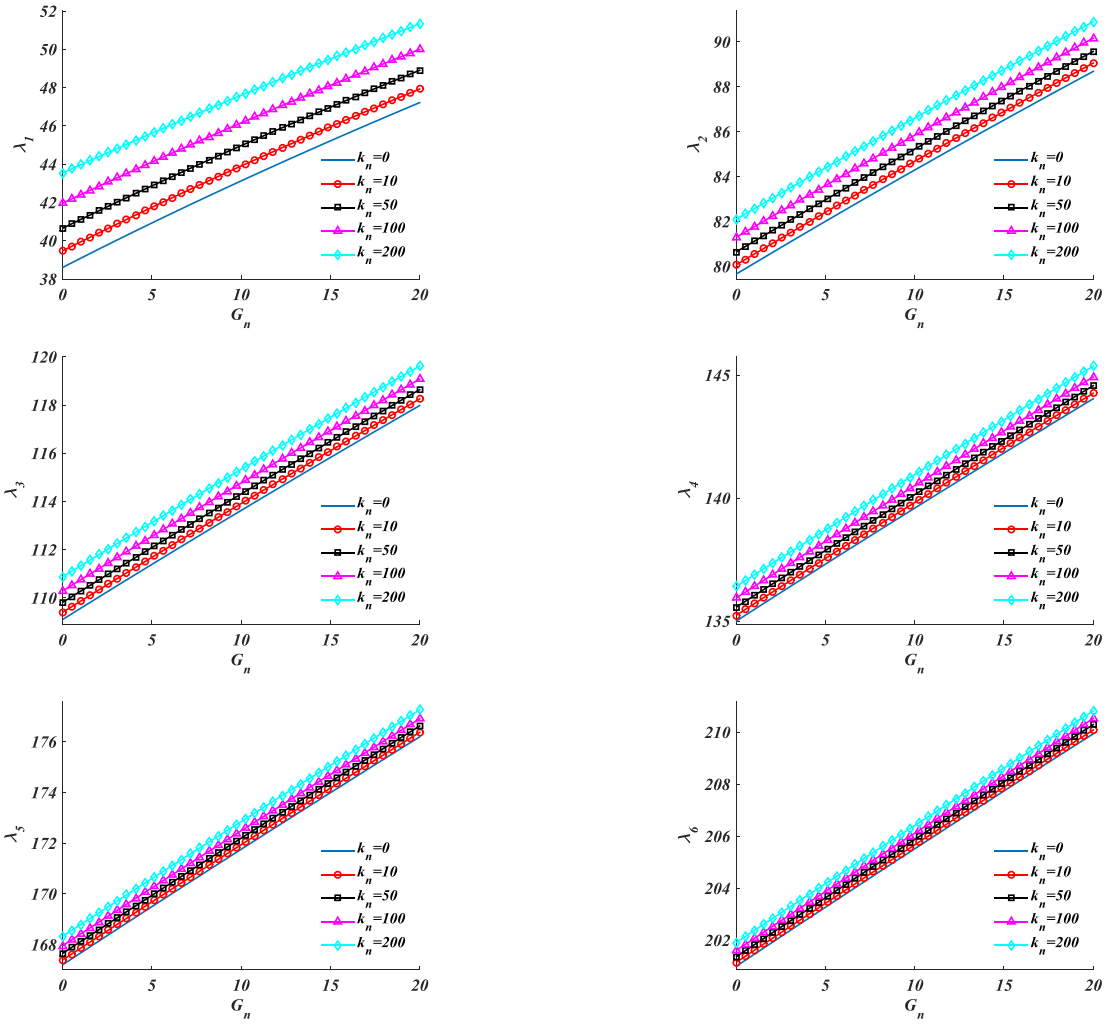

Fig. 5 First six natural frequencies of simply supported FG sector plate on foundation for various values of foundation coefficients (q=1, φ=0.2, α=π/2, η=0.1, c_n=0, N_{rr}=N_{tt}=N_{rt}=0)

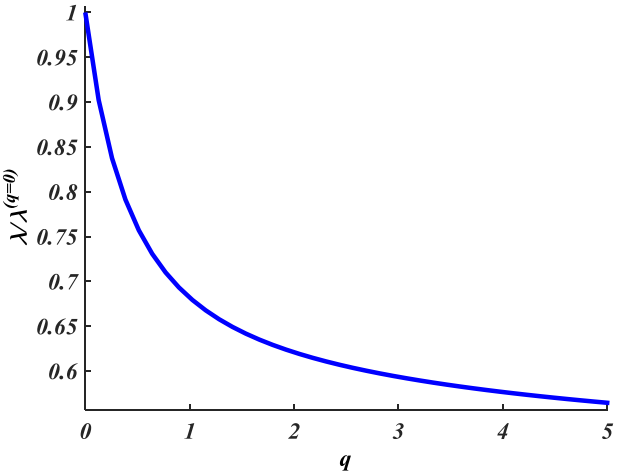

Fig. 4 Ratio of the natural frequencies presented in Table 3 to the corresponding values of the homogeneous ones (q=0)

decrease with increasing in value of the *q* that this result can be seen in Fig. 3. This figure shows that with increasing the value of the *q*, the modulus of elasticity decreases and mass density increases. An interesting result which can be derived from Table 3 is depicted in Fig. 4. This figure shows the ratio of the natural frequencies presented in Table 3, to the corresponding values of the homogeneous ones (*q=0*). It is concluded from Fig. 3 that this ratio is independent from number of mode and external boundary conditions and decreases with increase in value of q.

Fig. 5 depicts the effect of the k_n and G_n on the first six natural frequencies of FG sector plate. It is seen that both Winkler and Pasternak coefficients cause to increase in the value of the natural frequencies. This figure shows that the effect of this coefficients decreases in higher modes. It can be justified by increasing number of nodes and inflection points in higher modes.

The effect of the in-plane loads on the natural frequencies is investigated in Fig. 6. FGM annular sector plate resting on foundation and subjected to radial in-plane load is considered. Ratio of the first six frequencies to the corresponding values of a plate without radial in-plane load (Λ_i) are depicted versus the values of the dimensionless radial in-plane load; Similar graph is demonstrated in Fig. 7 for circumferential in-plane load. As shown in these figures for some boundary conditions, tensile loads increase all

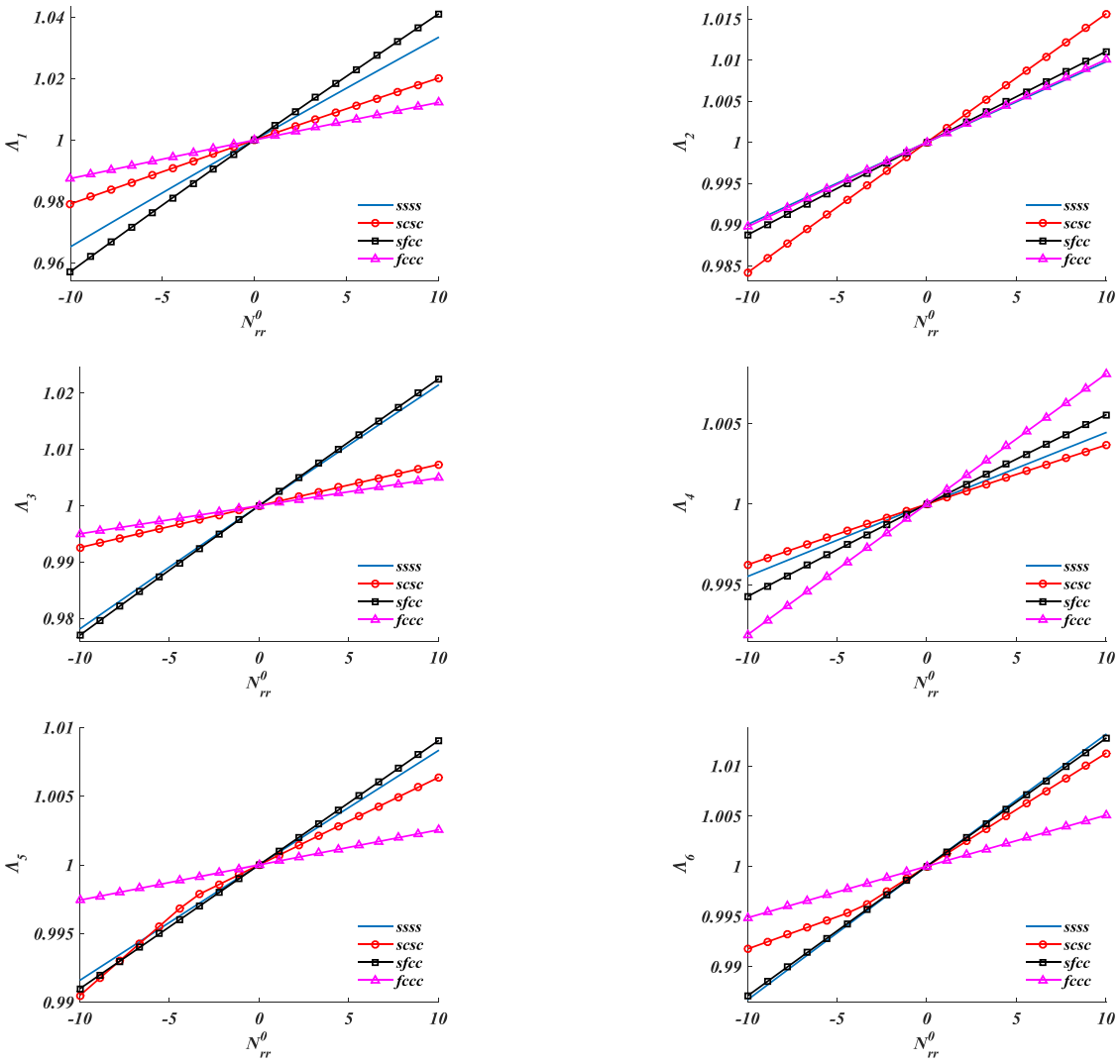

Fig. 6 First six natural frequencies of FG sector plate on foundation for various values of radial in-plane load (q=1, φ=0.3, α=π/3, η=0.05, k_n=100, G_n=10, c_n=0, $N_{\theta\theta}$=$N_{r\theta}$=0)

frequencies and compressive ones leads to decrease in all frequencies. It should be mentioned that as compressive loads lead first frequency to zero, corresponding form of buckling will be happened. In order to study about shear load, consider FGM annular sector plate resting on foundation and subjected to in-plane loads as $N^0{}_{rr}=N^0{}_{\theta\theta}=10$. Ratio of the first six frequencies to the corresponding values of a plate without shear in-plane load (Λ_i) are depicted in Fig. 8 versus the values of the dimensionless shear in-plane load; As shown shear force leads to either increase or decrease in frequencies; but this figure shows an interesting result that for plates whose radial boundary conditions are same, there is no difference in direction of the shear force and in other cases, direction of the shear force effects on the natural frequencies.

Table 6 shows the value of the $\Omega_i = \eta\lambda_i = a\omega_i\sqrt{12(1-\upsilon^2)\rho_m/E_m}$ for various values of thickness ration (η) and some boundary conditions. As shown, all of the natural frequencies increase with increasing in value of the thickness. Also, corresponding mode shapes are depicted in Fig. 9 for $\eta=0.05$. It should be mentioned that as value of the η increases, accuracy of the Kirchhoff's theory decreases.

In order to study about the effect of the damping of the foundation on the frequencies, FGM annular sector plate resting on a viscous foundation and subjected to in-plane loads is considered; Tables 7-8 show the real and imaginary parts of the first six dimensionless frequencies versus values of c_n for some boundary conditions. These tables reveal that as value of the damping coefficient increases, value of the frequencies decreases to zero and rate of the attenuation increases; As is anticipated, in comparison with higher modes, lower ones vanish for smaller values of damping coefficients. Because of increasing number of nodes in higher modes, the effect of the damping coefficients for higher frequencies is less than its effect on the lower ones. In order to propose a graphical view, Fig. 10 shows the variation of the ratio of the first six frequencies to the corresponding frequencies of a plate on a non-viscous foundation ($c_n=0$), denoted by (Λ_i) versus values of c_n for some boundary conditions.

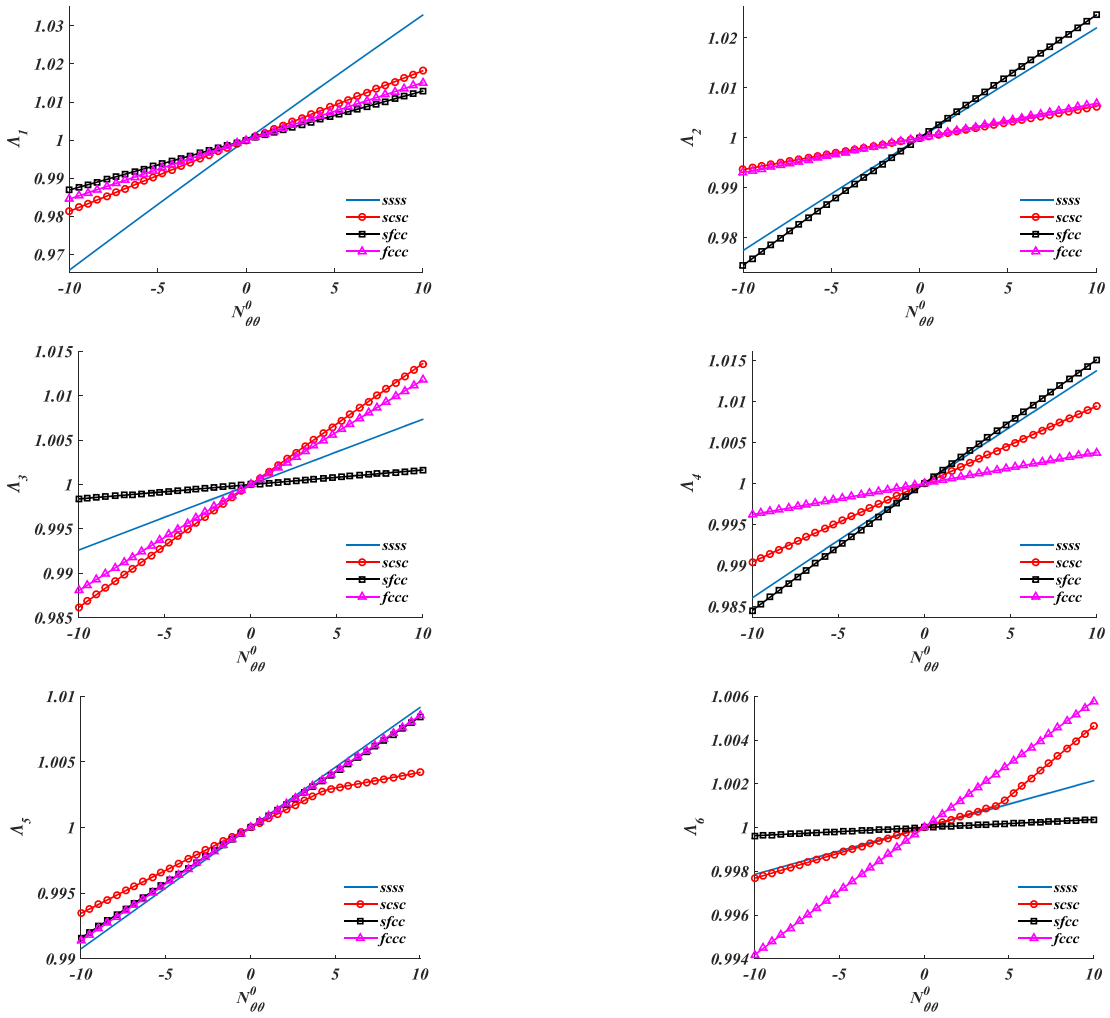

Fig. 7 First six natural frequencies of FG sector plate on foundation for various values of circumferential in-plane load (q=1, φ=0.3, α=π/3, η=0.05, k_n=100, G_n=10, c_n=0, N_{rr}= $N_{r\theta}$=0)

Table 6 Effect of the ratio of the thickness to the outer radius (η) on the first six natural frequencies of FG sector plate for some boundary conditions (q=1, φ=0.3, α=π/3, k_n=100, G_n=10, c_n=0, N_{rr}=$N_{\theta\theta}$=$N_{r\theta}$=10)

	η					η				
	0.005	0.01	0.02	0.05	0.1	0.005	0.01	0.02	0.05	0.1
	Ω_1					Ω_2				
CCCC	0.587789	1.175391	2.349284	5.847195	11.51389	1.103965	2.207140	4.407975	10.91140	21.09569
SCSC	0.479513	0.958883	1.916621	4.771644	9.40494	0.958194	1.915717	3.826069	9.472832	18.32691
FCSC	0.478109	0.956076	1.911018	4.757842	9.378718	0.925569	1.850534	3.696251	9.157592	17.75614
SFCF	0.271561	0.543089	1.085915	2.710194	5.387947	0.372583	0.745113	1.489806	3.717168	7.382510
	Ω_3					Ω_4				
CCCC	1.178397	2.355881	4.704486	11.63615	22.43879	1.783660	3.565089	7.11241	17.47899	33.02483
SCSC	0.973032	1.945392	3.885424	9.621259	18.62338	1.612077	3.222205	6.428881	15.80799	29.91957
FCSC	0.970638	1.940609	3.875904	9.59824	18.58211	1.458667	2.915863	5.820002	14.34936	27.38360
SFCF	0.693375	1.386509	2.771093	6.894314	13.55713	0.780434	1.560481	3.117869	7.741167	15.11718
	Ω_5					Ω_6				
CCCC	1.845161	3.687916	7.356677	18.06642	34.05926	2.039326	4.075687	8.127775	19.92017	37.32757
SCSC	1.660424	3.318735	6.620636	16.26498	30.68467	1.671932	3.341667	6.66585	16.36862	30.87096
FCSC	1.613018	3.224089	6.432661	15.81767	29.9406	1.661917	3.321757	6.626972	16.28626	30.77359
SFCF	0.918554	1.836616	3.669312	9.105492	17.74898	1.22277	2.444644	4.882133	12.08223	23.34146

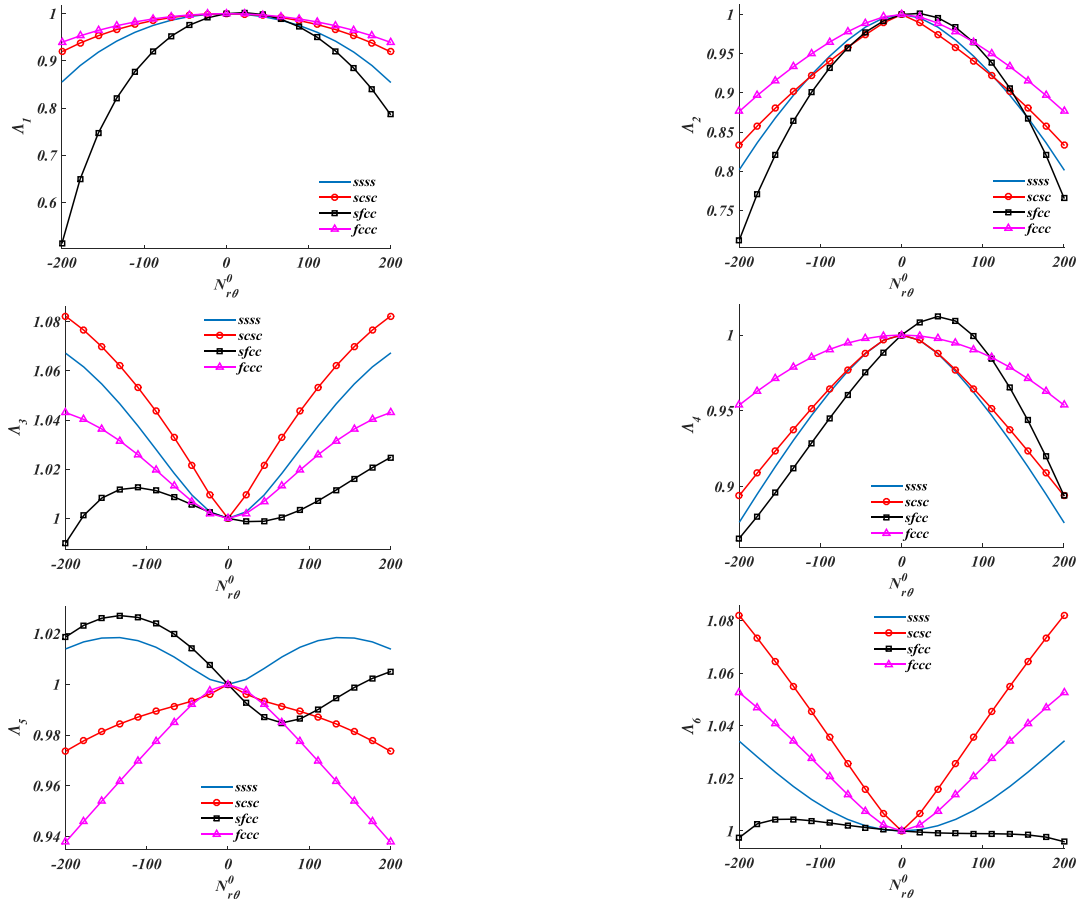

Fig. 8 First six natural frequencies of FG sector plate on foundation for various values of shear in-plane load (q=1, φ=0.3, α=π/3, η=0.05, k_n=100, G_n=10, c_n=0, N_{rr}=$N_{\theta\theta}$=10)

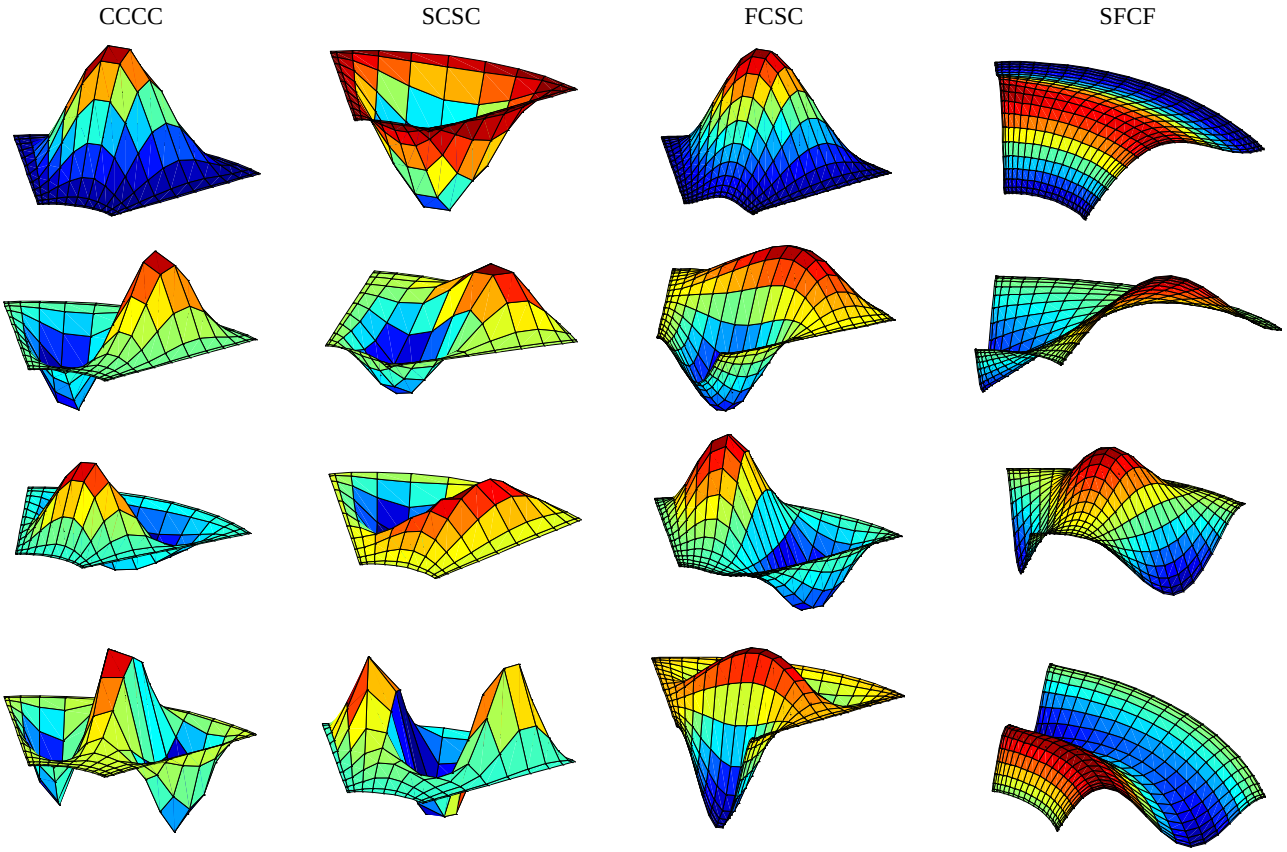

Fig. 9 Mode shapes of FG annular sector plate described in Table 6 for η=0.05

Table 7 Effect of the damping coefficient on the first six frequencies of FG sector plate for some boundary conditions (q=1, φ=0.2, α=π, η=0.05, k_n=100, G_n=10, $N_{rr}=N_{\theta\theta}=N_{r\theta}$=10)

c_n	0	10	30	70	120	0	10	30	70	120
			Im (λ_1)					Im (λ_2)		
SSSS	37.30479	36.66312	31.05614	0	0	48.97976	48.4947	44.42394	9.06868	0
CCCC	59.55212	59.15291	55.85662	34.99186	0	72.14819	71.82041	69.14222	53.78677	0
CSSC	44.07251	43.5312	38.93071	0	0	54.54698	54.11215	50.49886	25.69399	0
SSCC	50.35201	49.87894	45.91924	14.55719	0	64.97286	64.60852	61.61624	43.68134	0
			Im (λ_3)					Im (λ_4)		
SSSS	67.50955	67.16044	64.29927	47.47377	0	90.92381	90.66668	88.58275	77.32523	39.28578
CCCC	93.12486	92.87268	90.83007	79.83689	43.79471	120.1174	119.9234	118.3603	110.2126	87.88483
CSSC	72.50953	72.18479	69.5323	54.36196	0	96.21436	95.97156	94.00655	83.49063	50.3749
SSCC	87.02869	86.75868	84.56753	72.62682	28.5782	113.9121	113.7074	112.0568	103.4091	79.17132
			Im (λ_5)					Im (λ_6)		
SSSS	105.0544	104.8326	103.0411	93.57014	65.82476	118.0911	117.8948	116.3125	108.054	85.29324
CCCC	148.3023	148.1459	146.8891	140.4364	123.7698	151.4088	151.2563	150.0302	143.743	127.5751
CSSC	121.6877	121.4967	119.9576	111.9451	90.10351	124.1257	123.9391	122.4359	114.6245	93.49248
SSCC	129.2328	129.053	127.6053	120.1051	100.0637	144.4105	144.2504	142.9638	136.3483	119.1736

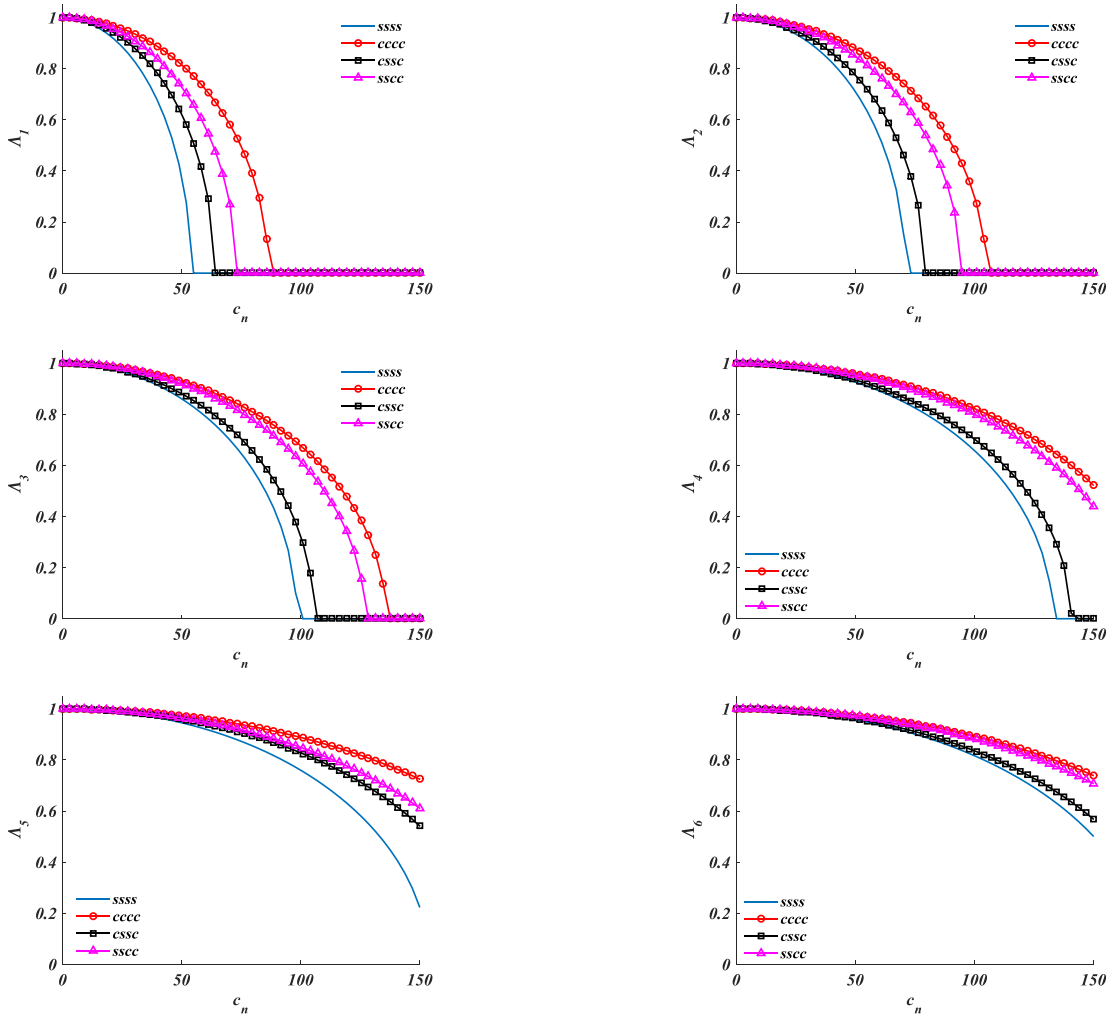

Fig. 10 Effect of the damping coefficient on the first six frequencies of FG sector plate for some boundary conditions (q=1, φ=0.2, α=π, η=0.05, k_n=100, G_n=10, $N_{rr}=N_{\theta\theta}=N_{r\theta}$=10)

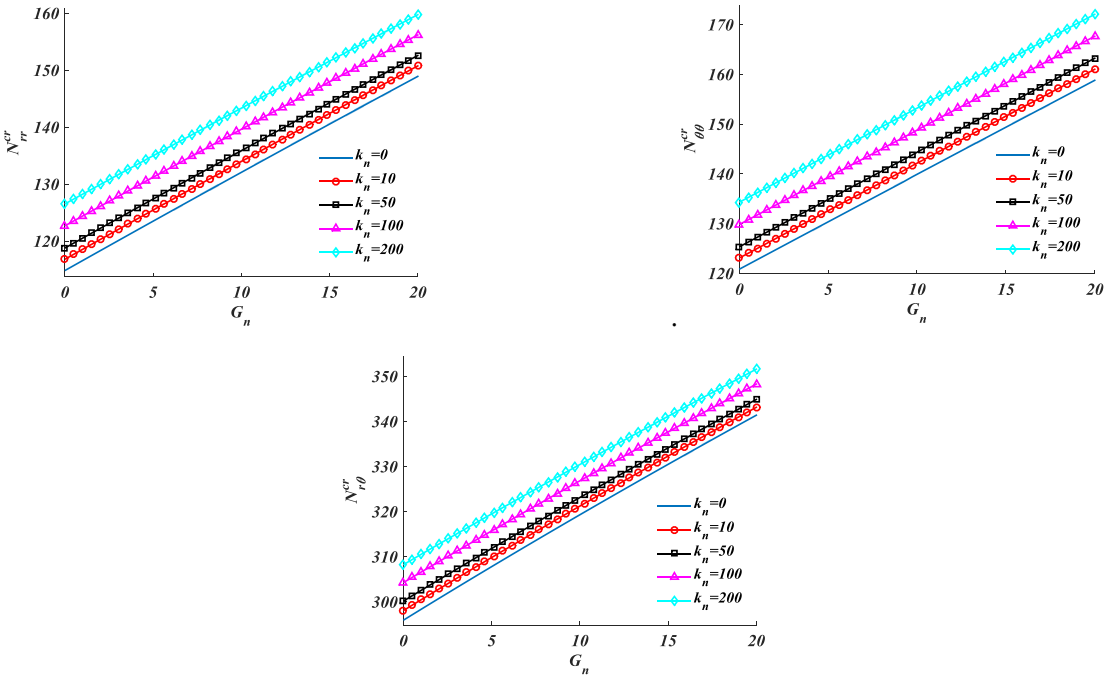

Fig. 11 Buckling loads of simply supported FG sector plate on foundation for various values of foundation coefficients (q=1, φ=0.3, α=π/3, η=0.05, c_n=0)

Table 8 Effect of the damping coefficient on the damping rate of the first six frequencies of FG sector plate for some boundary conditions (q=1, φ=0.2, α=π, η=0.05, k_n=100, G_n=10, N_{rr}=$N_{\theta\theta}$=$N_{r\theta}$=10)

c_n	0	10	30	70	120	0	10	30	70	120
			Re (λ_1)					Re (λ_2)		
SSSS	0	-6.88931	-20.6679	-	-	0	-6.87613	-20.6284	-48.1329	-
CCCC	0	-6.88391	-20.6517	-48.1874	-	0	-6.86955	-20.6087	-48.0869	-
CSSC	0	-6.88626	-20.6588	-	-	0	-6.87378	-20.6213	-48.1165	-
SSCC	0	-6.88597	-20.6579	-48.2018	-	0	-6.87114	-20.6134	-48.098	-
			Re (λ_3)					Re (λ_4)		
SSSS	0	-6.85682	-20.5704	-47.9977	-	0	-6.83321	-20.4996	-47.8325	-81.9986
CCCC	0	-6.84868	-20.546	-47.9408	-82.1846	0	-6.82339	-20.4702	-47.7638	-81.881
CSSC	0	-6.85478	-20.5643	-47.9835	-	0	-6.83108	-20.4932	-47.8176	-81.9731
SSCC	0	-6.85021	-20.5506	-47.9515	-82.2029	0	-6.82513	-20.4754	-47.7759	-81.9019
			Re (λ_5)					Re (λ_6)		
SSSS	0	-6.82293	-20.4688	-47.7605	-81.8751	0	-6.80613	-20.4184	-47.6429	-81.6735
CCCC	0	-6.80823	-20.4247	-47.6578	-81.6996	0	-6.79523	-20.3857	-47.5666	-81.5427
CSSC	0	-6.81566	-20.447	-47.7097	-81.7882	0	-6.80397	-20.4119	-47.6278	-81.6476
SSCC	0	-6.81521	-20.4456	-47.7065	-81.7828	0	-6.79668	-20.39	-47.5768	-81.5604

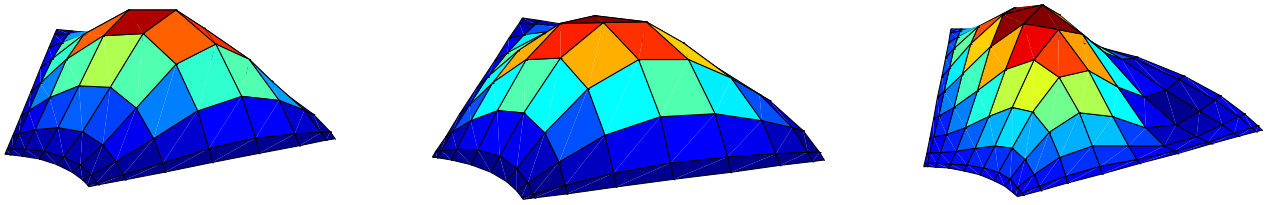

$N_r^{cr} = 137.5454$ $N_t^{cr} = 144.3611$ $N_{rt}^{cr} = 323.1171$

Fig. 12 Buckling modes of simply supported FG annular sector plate described in Fig. 9 for k_n=100, G_n=10

Results for the stability analysis are similar to the results of vibration analysis; In other words, each parameter which leads to increase (decrease) in natural frequencies, increases (decreases) the critical buckling loads, therefore, all results about the effect of the discussed parameters such as power-law exponent, ratio of radii, thickness of the plate, sector angle and Winkler and Pasternak coefficients of foundation on the natural frequencies, can be obtained for buckling loads. For example, the effect of elastic foundation on the critical buckling loads is investigated in Fig. 11 for a simply supported annular sector plate. As shown, both Winkler and Pasternak coefficients increase value of the critical buckling loads. Also, buckling modes are depicted in Fig. 12 for $k_n=100$ and $G_n=10$. This figure demonstrates the high accuracy of the proposed method in satisfying boundary conditions.

7. Conclusions

Vibration and stability analysis of FG annular thin sector plate resting on visco- elastic Pasternak foundation and subjected to normal and shear in-plane loads presented using GDQM. First, the governing equation was derived using Hamilton's principle and then was solved numerically using GDQM. Natural frequencies were obtained and compared with the reported results of other researchers. Comparison of the results showed the accuracy and versatility of the proposed GDQM. Moreover, the numerical results revealed that ratio of the frequency of FG annular sector plate to the corresponding values of homogeneous plate are independent from boundary conditions and frequency numbers. Numerical results also showed that natural frequencies increase with increasing the inner to outer radius ratio in most kinds of boundary conditions except for cases which inner edge is free. It also concluded for all boundary conditions that as value of the sector angle and value of the thickness ratio increase, the value of the frequencies decreases. Numerical examples revealed that the Winkler and Pasternak coefficients of the foundation increases value of frequencies and damping coefficient leads to decrease in them; It also was shown that all effects of foundation are stronger for lower modes.

Study about normal in-plane loads showed that for all boundary conditions, tensile loads increase all of the natural frequencies and compressive ones leads to decrease in them. Also, it was concluded that shear in-plane force leads to either increase or decrease in natural frequencies and it was shown that for plates whose radial boundary conditions are same, there is no difference in direct of the shear force and in other cases, direct of the shear force effects on the natural frequencies. Finally, it was shown that all parameters which lead to increase in the natural frequencies, increase the critical buckling loads and vice versa.

It is noted that the results of this work acceptable for thin plates and they can be improved by using more accurate plate theories like first order shear deformation theory (FSDT) or third order shear deformation theory (TSDT). It can be considered as a good proposal for next studies.

Acknowledgement

The authors would like to thank the referees for their valuable comments. Also, they are thankful to the University of Kashan for supporting this work by Grant No. 574602/10.

References

Abdelaziz, H.H., Ait Amar Meziane, M., Bousahla, A.A., Tounsi, A., Hassan, S. and Salim, A. (2017), "An efficient hyperbolic shear deformation theory for bending, buckling and free vibration of FGM sandwich plates with various boundary conditions", *Steel. Compos. Struct.*, **25**(6), 693-704. https://doi.org/10.12989/scs.2017.25.6.693.

Abualnour, M., Ahmed, H.M.S., Tounsi, A., Bedia, E.A.A. and Mahmoud S.R. (2018), "A novel quasi-3D trigonometric plate theory for free vibration analysis of advanced composite plates", *Compos. Struct.*, **184**, 688-697. https://doi.org/10.1016/j.compstruct.2017.10.047.

Adim, B., Hassaine Daouadji, T. and Abbes, B. (2016), "Buckling analysis of anti-symmetric cross-ply laminated composite plates under different boundary conditions", *Appl. Mech.*, **52**(6), 661-676. https://doi.org/10.1007/s10778-016-0787-x.

Afshari, H. and Irani Rahaghi, M. (2018), "Whirling analysis of multi-span multi-stepped rotating shafts", *J. Braz. Soci. Mech. Sci. Eng.*, **40**(9), 424. https://doi.org/10.1007/s40430-018-1351-x.

Afshari, H. and Torabi, K. (2017), "A parametric study on flutter analysis of cantilevered trapezoidal FG sandwich plates", *AUT. J. Mech. Eng.*, **1**(2), 191-210 . http://dx.doi.org/10.22060/mej.2017.12329.5314.

Akgöz, B. and Civalek, O. (2011), "Buckling analysis of cantilever carbon nanotubes using the strain gradient elasticity and modified couple stress theories", *J. Comput. Theory. Nano. Sci.*, **8**, 1821-1827. https://doi.org/10.1166/jctn.2011.1888.

Alipour, M.M. (2016), "Effects of elastically restrained edges on FG sandwich annular plates by using a novel solution procedure based on layerwise formulation", *Arch. Civil. Mech. Engin.*, **16**(4), 678-694. https://doi.org/10.1016/j.acme.2016.04.015.

Ansari, R. and Torabi, J. (2016), "Nonlocal vibration analysis of circular double-layered graphene sheets resting on an elastic foundation subjected to thermal loading", *Acta Mechanica Sinica*, **32**(5), 841-853. https://doi.org/10.1007/s10409-016-0574-2.

Bakhadda, B., Bouiadjra, M.B., Bourada, F., Bousahla, A.A., Tounsi, A. and Hassan, S. (2018), "Dynamic and bending analysis of carbon nanotube-reinforced composite plates with elastic foundation", *Wind. Struct.*, **27**(5), 311-324. https://doi.org/10.12989/was.2018.27.5.311.

Baltacıoglu, A.K., Akgoz, B. and Civalek, O. (2010), "Nonlinear static response of laminated composite plates by discrete singular convolution method", *Compos. Struct.*, **93**, 53-161. https://doi.org/10.1016/j.compstruct.2010.06.005.

Behera, L. and Chakraverty, S. (2015), "Application of differential quadrature method in free vibration analysis of nano beams based on various nonlocal theories", *Comput. Math. Appl.*, **69**(12), 1444-1462. https://doi.org/10.1016/j.camwa.2015.04.010.

Belabed, Z., Bousahla, A.A., Ahmed, H.M.S., Tounsi, A. and Hassam, S. (2018), "A new 3-unknown hyperbolic shear deformation theory for vibration of functionally graded sandwich plate", *Earthquake. Struct.*, **14**(2), 103-115. https://doi.org/10.12989/eas.2018.14.2.103.

Bellman, R., Kashef, B.G. and Casti, J. (1972), "Differential quadrature: A technique for the rapid solution of nonlinear

partial differential equations", *J. Comput. Phys.*, **10**(1), 40-52. https://doi.org/10.1016/0021-9991(72)90089-7.

Benchohra, M., Driz, H., Bekora, A., Tounsi, A., Bedia, E.A.A. and Hassan, S. (2018), "A new quasi-3D sinusoidal shear deformation theory for functionally graded plates", *Struct. Eng. Mech.*, **65**(1), 19-31. https://doi.org/10.12989/sem.2018.65.1.019.

Bennoun, M., Ahmed, H.M.S. and Tounsi, A. (2016), "A novel five variable refined plate theory for vibration analysis of functionally graded sandwich plates", *Mech. Adv. Mater.Struct.*, **23**(4), 423-431. https://doi.org/10.1080/15376494.2014.984088.

Bert, C.W., Jang, S.K. and Striz, A.F. (1988), "Two new approximate methods for analyzing free vibration of structural components", *AIAA J.*, **26**(5), 612-618.

Bert, C.W. and Malik, M. (1996), "Differential quadrature method in computational mechanics: A review", *Appl. Mech. Rev.*, **49**(1), 1-28. https://doi.org/10.1115/1.3101882.

Besseghier, A., Ahmed, H.M.S., Tounsi, A. and Hassan, S. (2017), "Free vibration analysis of embedded nanosize FG plates using a new nonlocal trigonometric shear deformation theory", *Smart. Struct. Syst.*, **19**(6), 601-614. https://doi.org/10.12989/sss.2017.19.6.601.

Bhaskara, L. and Kameswara, C. (2014), "Buckling of elastic circular plates with an elastically restrained edges against rotation and internal elastic ring support", *Int. Appl. Mech.*, **51**(4), 480-488. https://doi.org/10.1007/s10778-015-0709-3.

Bouafia, K., Abdelhakim, K., Ahmed, H.M.S., Benzair, A. and Tounsi, A. (2017), "A nonlocal quasi-3D theory for bending and free flexural vibration behaviors of functionally graded nanobeams", *Smart. Struct. Sys.*, **19**(2), 115-126. https://doi.org/10.12989/sss.2017.19.2.115.

Bouhadra, A., Tounsi, A., Bousahla, A.A., Benyoucef, S. and Hassan, S. (2018), "Improved HSDT accounting for effect of thickness stretching in advanced composite plates", *Struct. Eng. Mech.*, **66**(1), 61-73.

Bounouara, F., Benrahou, K.H., Belkorissat, I. and Tounsi, A. (2016), "A nonlocal zeroth-order shear deformation theory for free vibration of functionally graded nanoscale plates resting on elastic foundation", *Steel. Compos. Struct.*, **20**(2), 227-249. https://doi.org/10.12989/scs.2016.20.2.227.

Bourada, F., Amara, K., Bousahla, A.A., Tounsi, A. and Hassan, S. (2018), "A novel refined plate theory for stability analysis of hybrid and symmetric S-FGM plates", *Struct. Engin. Mech.*, **68**(6), 661-675. https://doi.org/10.12989/sem.2018.68.6.661.

Bourada, F., Bousahla, A.A., Bourada, M., Azzaz, A., Amina, Z. and Tounsi, A. (2019), "Dynamic investigation of porous functionally graded beam using a sinusoidal shear deformation theory", *Wind. Struct.*, **28**(1), 19-30. https://doi.org/10.12989/was.2019.28.1.019.

Bousahla, A.A., Ahmed, H.M.S., Tounsi, A. and Bedia, E.A. (2014), "A novel higher order shear and normal deformation theory based on neutral surface position for bending analysis of advanced composite plates", *Int. J. Comput. Method.*, **11**(6), 1350082. https://doi.org/10.1142/S0219876213500825.

Bousahla, A.A., Benyoucef, S., Tounsi, A. and Hassan, S. (2016), "On thermal stability of plates with functionally graded coefficient of thermal expansion", *Struct. Eng. Mech.*, **60**(2), 313-335. https://doi.org/10.12989/sem.2016.60.2.313.

Cho, J.R. and Oden, J.T. (2000), "Functionally graded material: a parametric study on thermal-stress characteristics using the Crank–Nicolson–Galerkin scheme", *Comput. Method. Appl. Mech. Eng.*, **188**(1-3), 17-38. https://doi.org/10.1016/S0045-7825(99)00289-3.

Civalek, O. (2006), "The determination of frequencies of laminated conical shells via the discrete singular convolution method", *J. Mech. Mater. Struct.*, **1**, 163-182. http://dx.doi.org/10.2140/jomms.2006.1.163.

Civalek, O. (2008), "Vibration analysis of conical panels using the method of discrete singular convolution", *Commun. Numerical. Method. Engin.*, **24**, 169-181. https://doi.org/10.1002/cnm.961.

Civalek, O. (2013), "Nonlinear dynamic response of laminated plates resting on nonlinear elastic foundations by the discrete singular convolution-differential quadrature coupled approaches", *Compos. Part B.*, **50**, 171–179. https://doi.org/10.1016/j.compositesb.2013.01.027.

Civalek, O. (2017), "Free vibration of carbon nanotubes reinforced (CNTR) and functionally graded shells and plates based on FSDT via discrete singular convolution method", *Compos. Part B.*, **111**, 45-59. https://doi.org/10.1016/j.compositesb.2016.11.030.

Demir, C., Mercan, K. and Civalek, O. (2016), "Determination of critical buckling loads of isotropic, FGM and laminated truncated conical panel", *Compos. Part B.*, **94**, 1-10. https://doi.org/10.1016/j.compositesb.2016.03.031.

Dung, D.V., NGA, N.T. and Hoa, L.K. (2017), "Nonlinear stability of functionally graded material (FGM) sandwich cylindrical shell reinforced by FGM stiffeners in thermal environment", *Appl. Math. Mech.*, **38**(5), 647-670. https://doi.org/10.1007/s10483-017-2198-9.

El-Haina, F., Bekora, A., Bousahla, A.A., Tounsi, A. and Hassan, S. (2017), "A simple analytical approach for thermal buckling of thick functionally graded sandwich plates", *Struct. Eng. Mech.*, **63**(5), 585-595. https://doi.org/10.12989/sem.2017.63.5.585.

Fadaee, M. (2015), "A novel approach for free vibration of circular/ annular sector plates using Reddy's third order shear deformation theory", *Meccanica*, **50**(9), 2325-2351. https://doi.org/10.1007/s11012-015-0158-4.

Fourn, H., Hassen, A.A., Bourada, M., Bousahla, A.A., Tounsi, A. and Hassan, S. (2018), "A novel four variable refined plate theory for wave propagation in functionally graded material plates", *Steel. Compos. Struct.*, **27**(1), 109-122. https://doi.org/10.12989/scs.2018.27.1.109.

Hichem, B., Bakora, A., Tounsi, A., Bousahla, A.A. and Hassa, S. (2017), "An efficient and simple four variable refined plate theory for buckling analysis of functionally graded plates", *Steel. Compos. Struct.*, **25**(3), 257-270. https://doi.org/10.12989/scs.2017.25.3.257.

Karami, B., Janghorban, M. and Tounsi, A. (2018), "Variational approach for wave dispersion in anisotropic doubly-curved nanoshells based on a new nonlocal strain gradient higher order shell theory", *Thin-Walled Struct.*, **129**, 251-264. https://doi.org/10.1016/j.tws.2018.02.025.

Kim, C.S. and Dickinson, S.M. (1989), "On the free, transverse vibration of annular and circular, thin, sectorial plates subject to certain complicating effects", *J. Sound. Vib.*, **134**(3), 407-421. https://doi.org/10.1016/0022-460X(89)90566-X.

Koizumi, M. (1997), "FGM activities in Japan", *Compos. Engin.*, **28**(1-2), 1-4. https://doi.org/10.1016/S1359-8368(96)00016-9.

Kumar, Y. and Lal, R. (2013), "Prediction of frequencies of free axisymmetric vibration of two-directional functionally graded annular plates on Winkler foundation", *Europ. J. Mech. A/Solids.*, **42**, 219-228. https://doi.org/10.1016/j.euromechsol.2013.06.001.

Liang, X., Kou, H.L., Wang, L., Palmer, A.C., Wang, Z. and Liu, M. (2015), "Three-dimensional transient analysis of functionally graded material annular sector plate under various boundary conditions", *Compos. Struct.*, **132**, 584-596. https://doi.org/10.1016/j.compstruct.2015.05.066.

Long, N.V., Quoc, T.H. and Tu, T.M. (2016), "Bending and free vibration analysis of functionally graded plates using new eight-unknown shear deformation theory by finite-element method", *J. Adv. Struct. Engin.*, **8**(4), 391-399. https://doi.org/10.1007/s40091-016-0140-y.

Mehrabian, M. and Golmakani, M.E. (2015), "Nonlinear bending analysis of radial-stiffened annular laminated sector plates with dynamic relaxation method", *Comput. Math. Appl.*, **69**(10), 1272-1302. https://doi.org/10.1016/j.camwa.2015.03.021.

Menasria, A., Bouhadra, A., Tounsi, A., Bousahla, A.A. and Mahmoud, S.R. (2017), "A new and simple HSDT for thermal stability analysis of FG sandwich plates", *Steel. Compos. Struct.*, **25**(2), 157-175. https://doi.org/10.12989/scs.2017.25.2.157.

Meksi, R., Benyoucef, S., Mahmoudi, A., Tounsi, A., Bedia, E.A.A. and Hassan, S. (2019), "An analytical solution for bending, buckling and vibration responses of FGM sandwich plates", *J. Sandw. Struct. Mater.*, **21**(2), 727-757. https://doi.org/10.1177%2F1099636217698443.

Mercan, K. and Civalek, O. (2016), "DSC method for buckling analysis of boron nitride nanotube (BNNT) surrounded by an elasticmatrix", *Compos. Struct.*, **143**, 300-309. https://doi.org/10.1016/j.compstruct.2016.02.040.

Mercan, K. and Civalek, O. (2017), "Buckling analysis of Silicon carbide nanotubes (SiCNTs) with surface effect and nonlocalelasticity using the method of HDQ", *Compos. Part B.*, **114**, 34-45. https://doi.org/10.1016/j.compositesb.2017.01.067.

Meziane, M.A.A., Abdelaziz, H.H. and Tounsi, A. (2014), "An efficient and simple refined theory for buckling and free vibration of exponentially graded sandwich plates under various boundary conditions", *J. Sandw. Struct. Mater.*, **16**(3), 293-318. https://doi.org/10.1177/1099636214526852.

Mirsalehi, M., Azhari, M. and Amoushahi, H. (2017), "Buckling and free vibration of the FGM thin micro-plate based on the modified strain gradient theory and the spline finite strip method", *Europ. J. Mech. A/Solids.*, **61**, 1-13. https://doi.org/10.1016/j.euromechsol.2016.08.008.

Mohammadimehr, M. and Mehrabi, M. (2018), "Electro-thermo-mechanical vibration and stability analyses of double-bonded micro composite sandwich piezoelectric tubes conveying fluid flow", *Appl. Math. Model.*, **60**, 255-272. https://doi.org/10.1016/j.apm.2018.03.008.

Mohammadimehr, M., Shabani Nejad, E. and Mehrabi, M. (2018), "Buckling and Vibration Analyses of MGSGT double-bonded micro composite sandwich SSDT plates reinforced by CNTs and BNNTs with isotropic foam & flexible transversely orthotropic cores", *Struct. Engin. Mech.*, **65**(4), 491-504. https://doi.org/10.12989/sem.2018.65.4.491.

Mohammadimehr, M. and Mehrabi, M. (2017), "Stability and vibration analysis of double-bonded micro composite sandwich cylindrical shells conveying fluid flow", *Appl. Math. Model.*, **47**, 685-709. https://doi.org/10.1016/j.apm.2017.03.054.

Mohammadimehr, M., Farahi, M.J. and Alimirzaei, S. (2016), "Vibration and wave propagation analysis of twisted micro-beam using strain gradient theory", *Appl. Math. Mech.*, **37**(10), 1375-1392. https://doi.org/10.1007/s10483-016-2138-9.

Mohammadimehr, M., Saidi, A.R., Ghorbanpour Arani, A., Arefmanesh, A. and Han Q. (2010), "Torsional buckling of a DWCNT embedded on winkler and pasternak foundations using nonlocal theory", *J. Mech. Sci. Tech.*, **24**(6), 1289-1299. https://doi.org/10.1007/s12206-010-0331-6.

Mohammadimehr, M., BabaAkbar Zarei, H., Parakandeh, A., Ghorbanpour Arani, A. (2017), "Vibration analysis of double-bonded sandwich microplates with nanocomposite facesheets reinforced by symmetric and un-symmetric distributions of nanotubes under multi physical fields", *Struct. Engin. Mech.*, **64** (3), 361-379. https://doi.org/10.12989/sem.2017.64.3.361.

Mohammadimehr M., Saidi A.R., Ghorbanpour Arani A., Arefmanesh A. and Han Q. (2011) "Buckling analysis of double-walled carbon nanotubes embedded in an elastic medium under axial compression using non-local Timoshenko beam theory", *Proc. IMechE, Part C: J. Mech. Eng. Sci.*, **225**(2), 498-506. https://doi.org/10.1177/2041298310392861.

Ghorbanpour Arani A., Rahnama Mobarakeh M., Shams Sh. and Mohammadimehr M. (2012) "The effect of CNT volume fraction on the magneto-thermo-electro-mechanical behavior of smart nanocomposite cylinder", *J. Mech. Sci. Technol.* **26**(8), 2565-2572. https://doi.org/10.1007/s12206-012-0639-5.

Ghorbanpour Arani, A., Mohammadimehr, M., Saidi, A.R., Shogaei, S. and Arefmanesh, A. (2011), "Thermal buckling analysis of double-walled carbon nanotubes considering the small-scale length effect", *Proc. IMechE, Part C, J. Mech. Eng. Sci.*, **225**(1), 248-256. https://doi.org/10.1177/09544062JMES1975.

Mohammadimehr, M., Rostami, R., Arefi, M., 2016, "Electro-elastic analysis of a sandwich thick plate considering FG core and composite piezoelectric layers on Pasternak foundation using TSDT", *Steel Compos. Struct.*, **20**(3), 513-544. https://doi.org/10.12989/scs.2016.20.3.513.

Mohammadimehr, M. and Rahmati, A.H. (2013), "Small scale effect on electro-thermo-mechanical vibration analysis of single-walled boron nitride nanorods under electric excitation", *J. Eng. Environ. Sci.*, **37**(1), 1-15.

Mohammadimehr M. and Shahedi S. (2017) "High-order buckling and free vibration analysis of two types sandwich beam including AL or PVC-foam flexible core and CNTs reinforced nanocomposite face sheets using GDQM", *Compos. Part B: Eng.*, **108**, 91-107. https://doi.org/10.1016/j.compositesb.2016.09.040.

Ghorbanpour Arani, A., Hashemian, M., Loghman, A. and Mohammadimehr, M. (2011), "Study of dynamic stability of the double-walled carbon nanotubes under axial loading embedded in an elastic medium by the energy method", *J. Appl. Mech. Technical Physics*, **52**(5), 815-824. https://doi.org/10.1134/S0021894411050178.

Powmya, A. and Narasimhan, M.C. (2015), "Free vibration analysis of axisymmetric laminated composite circular and annular plates using Chebyshev collocation", *Int. J. Adv. Struct. Engin.*, **7**(2), 129-141. https://doi.org/10.1007/s40091-015-0087-4.

Reddy, J.N. (2002), *Energy Principles and Variational Methods in Applied Mechanics (2nd edition)*, John Wiley & Sons Inc, New Jersey, USA.

Satouri, S., Asanjarani, A. and Satouri, A. (2015), "Natural Frequency Analysis of 2D-FGM Sectorial Plate with Variable Thickness Resting on Elastic Foundation Using 2D-DQM", *Int. J. Appl. Mech.*, **7**(2). https://doi.org/10.1142/S1758825115500301.

Shirmohammadi, F. and Bahrami, S. (2018), "Dynamic response of circular and annular circular plates using spectral element method", *Appl. Math. Model.*, **53**, 156-166. https://doi.org/10.1016/j.apm.2017.08.014.

Swaminathan, K. and Sangeetha, D.M. (2017), "Thermal analysis of FGM plates – A critical review of various modelling techniques and solution methods", *Compos. Struct.*, **160**, 43-60. https://doi.org/10.1016/j.compstruct.2016.10.047.

Talebitooti, M. (2013), "Three-dimensional free vibration analysis of rotating laminated conical shells: layerwise differential quadrature (LW-DQ) method", *Arch. Appl. Mech.*, **83**(5),765-781. https://doi.org/10.1007/s00419-012-0716-3.

Thang, P.T., Nguyen-Thoi, T. and Lee, J. (2016), "Closed-form expression for nonlinear analysis of imperfect sigmoid-FGM plates with variable thickness resting on elastic medium", *Compos. Struct.*, **143**, 143-150. https://doi.org/10.1016/j.compstruct.2016.02.002.

Torabi, K. and Afshari, H. (2017a), "Vibration analysis of a cantilevered trapezoidal moderately thick plate with variable thickness", *Eng. Solid. Mech.*, **5**(1), 71-92 . http://dx.doi.org/10.5267/j.esm.2016.7.001.

Torabi, K., Afshari, H. and Haji Aboutalebi, F. (2017b), "Vibration and flutter analyses of cantilever trapezoidal honeycomb sandwich plates", *J. Sandw. Struct. Mater.* https://doi.org/10.1177/1099636217728746.

Torabi, K. and Afshari, H. (2016), "Generalized differential quadrature method for vibration analysis of cantilever trapezoidal FG thick plate", *J. Solid. Mech.*, **9**(1), 184-203.

Torabi, K., Afshari, H. and Haji Aboutalebi, F. (2014a), "A DQEM for transverse vibration analysis of multiple cracked non-uniform Timoshenko beams with general boundary conditions", *Comput. Math. Appl.*, **67**(3), 527-541. https://doi.org/10.1016/j.camwa.2013.11.010.

Torabi, K., Afshari, H. and Heidari-Rarani, M. (2014b), "Free vibration analysis of a rotating non-uniform blade with multiple open cracks using DQEM", *Uni. J. Mech. Eng.*, **2**(3), 101-111. https://doi.org/10.13189/ujme.2014.020304.

Torabi, K., Afshari, H. and Heidari-Rarani, M. (2013), "Free vibration analysis of a non-uniform cantilever Timoshenko beam with multiple concentrated masses using DQEM", *Eng. Solid. Mech.*, **1**(1), 9-20 . http://dx.doi.org/10.5267/j.esm.2013.06.002.

Wang, Y.G., Song, H.F., Lin, W.H. and Xu, L. (2017), "Large deflection analysis of functionally graded circular microplates with modified couple stress effect", *J. Braz. Soci. Mech. Sci. Engin.*, **39**(3), 981-991. https://doi.org/10.1007/s40430-016-0564-0.

Wu, Ch.P., Li, W.Ch. (2017), "Free vibration analysis of embedded single-layered nanoplate and graphene sheets by using the multiple time scale method", *Comput. Math. Appl*, **73**(5), 838-854. https://doi.org/10.1016/j.camwa.2017.01.014.

Wu, Y., Xing, Y. and Liu, B. (2018), "Analysis of isotropic and composite laminated plates and shells using a differential quadrature hierarchical finite element method", *Compos. Struct.*, **205**, 11-25. https://doi.org/10.1016/j.compstruct.2015.07.101.

Xiang, Y., Ma, Y.F., Kitiornchai, S., Lim, C.W. and Lau, C.W.H. (2002), "Exact solutions for vibration of cylindrical shells with intermidiate ring supports", *Int. J. Mech. Sci.*, **44**, 1907-1924. https://doi.org/10.1016/S0020-7403(02)00071-1.

Yahia, S.A., Hassen, A.A., Ahmed, H.M.S. and Tounsi, A. (2015), "Wave propagation in functionally graded plates with porosities using various higher-order shear deformation plate theories", *Struct. Eng. Mech.*, **53**(6), 1143-1165. http://dx.doi.org/10.12989/sem.2015.53.6.1143.

Yakhno, V.G., Ozdek, D. (2014), "Computation of the Green's function for the transverse vibration of a composite circular membrane", *J. Engin. Math*, **87**(1), 187-205. https://doi.org/10.1007/s10665-013-9673-2.

Younsi, A., Tounsi, A., Zaoui, F.Z., Bousahla, A.A. and Mahmoud, S.R. (2018), "Novel quasi-3D and 2D shear deformation theories for bending and free vibration analysis of FGM plates", *Geomech. Engin.*, **14**(6), 519-532. https://doi.org/10.12989/gae.2018.14.6.519.

Yousefitabar, M. and Matapouri, M.Kh. (2017), "Thermally induced buckling of thin annular FGM plates", *J. Braz. Soci, Mech. Sci. Engin*, **39**(3), 969-980. https://doi.org/10.1007/s40430-016-0555-1.

Zemri, A., Ahmed, H.M.S., Bousahla, A.A. and Tounsi, A. (2015), "A mechanical response of functionally graded nanoscale beam: an assessment of a refined nonlocal shear deformation theory beam theory", *Int. J. Struct. Eng. Mech.*, **54**(4), 693-710. https://doi.org/10.12989/sem.2015.54.4.693.

Zhong, H. and Yu, T. (2009), "A weak form quadrature element method for plane elasticity problems", *Appl. Math. Model.*, **33**(10), 3801-3814. https://doi.org/10.1016/j.apm.2008.12.007.

Zhou, Z.H., Wong, K.W., Xu, X.S. and Leung, A.Y.T. (2011), "Natural vibration of circular and annular thin plates by Hamiltonian approach", *J. Sound. Vib*, **330**(5), 1005–1010. https://doi.org/10.1016/j.jsv.2010.09.015.